© 2018. Published by The Company of Biologists Ltd | Development (2018) 145, dev168708. doi:10.1242/dev.168708

CORRECTION

Correction: Combinatorial actions of Tgfβ and Activin ligands promote oligodendrocyte development and CNS myelination (doi:10.1242/dev.106492)

Dipankar J. Dutta, Andleeb Zameer, John N. Mariani, Jingya Zhang, Linnea Asp, Jimmy Huynh, Sean Mahase, Benjamin M. Laitman, Azeb Tadesse Argaw, Nesanet Mitiku, Mateusz Urbanski, Carmen V. Melendez-Vasquez, Patrizia Casaccia, Fernand Hayot, Erwin P. Bottinger, Chester W. Brown and Gareth R. John

Development was made aware by a reader of potential duplication of data in Fig. 3 and Fig. S3 of Development (2014) **141**, 2414-2428 (doi:10.1242/dev.106492).

The journal contacted the authors who said that some of the bands in the western blots in Fig. 3 and Fig. S3 were manipulated during figure compilation. After discussion with the corresponding author, Development referred this matter to Icahn School of Medicine at Mount Sinai (ISMMS), who investigated and concluded that: "The main conclusions of the manuscript are supported by the data obtained utilizing other methodologies, including immunohistochemistry." Development's editorial policies state that: "Should an error appear in a published article that affects scientific meaning or author credibility but does not affect the overall results and conclusions of the paper, our policy is to publish a Correction…" and that a Retraction should be published when "…a published paper contain[s] one or more significant errors or inaccuracies that change the overall results and conclusions of a paper…". The journal follows the guidelines of the Committee on Publication Ethics (COPE), which state: "Retraction should usually be reserved for publications that are so seriously flawed (for whatever reason) that their findings or conclusions should not be relied upon".

The standards of figure assembly and data presentation in this paper fall short of good scientific practice. However, given that the ISMMS declared that the conclusions of the paper were not affected by the manipulations, the appropriate course of action – according to COPE guidelines – is to publish a Correction, which Development has made as detailed as possible. The corresponding author has provided the journal with the original scans of the relevant blots.

In the Mbp blot in Fig. 3C, lanes were rearranged to match the order of samples on the other blots without an appropriate explanation. These splices are now indicated with black lines in the new figure panel. The control actin blot in Fig. 3C was compressed vertically when the figure was prepared. The uncompressed blot is shown below, along with a new densitometric analysis in Fig. 3D based on these bands.

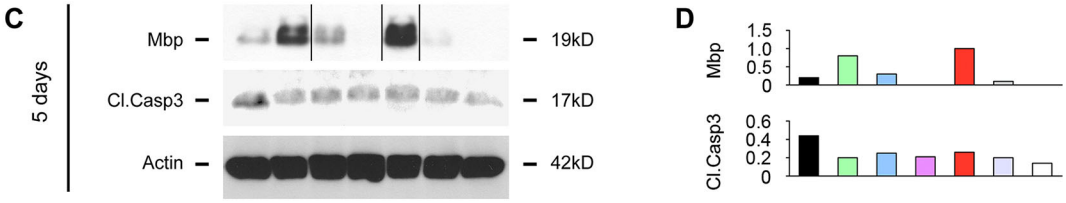

Fig. 3. Tgfβ1, ActB and co-treatment elicit distinct signaling and functional outcomes in OLPs. (C,D) Immunoblotting (C) and densitometry (D) of primary OLPs plated into serum-free media and exposed to 50 ng/ml Tgfβ1, ActB and/or Bmp4 for 5 days. Data accompany morphometric timecourse analyses in OLPs in E-J and supplementary material Fig. S4E-G. At 5 days, caspase-3 cleavage (a marker of apoptotic activity) was decreased in OLP cultures exposed to Tgfβ or ActB alone or together. Mbp expression (mature oligodendrocytes) was enhanced in ActB-treated and co-treated cultures. Bmp alone or in combination with Tgfβ or ActB abrogated Mbp expression.

The order of the lanes was incorrect in the P-GSK3α/β(S21/S9) blot in Fig. S3B. The correct order is shown in the new figure below, with lines indicating where lanes have been spliced. The investigation also showed that bands from the original P-GSK3α/β(S21/S9) blot were rearranged and duplicated in the actin blot. The correct actin blot for Fig. S3B was located and is shown in the new figure. Readers should note that the P-p44/42(T202/Y204) blot in Fig. S3B has also been replaced because the original blot was inappropriately over-contrasted. On the basis of these changes, a new densitometric analysis was carried out and is reported in Fig. S3C-J. In addition, the actin loading control blot in Fig. S3K was duplicated from Fig. 3A. The correct actin blot for Fig. S3K was located and is shown in the new figure below.

Development (2018) 145, dev168708. doi:10.1242/dev.168708

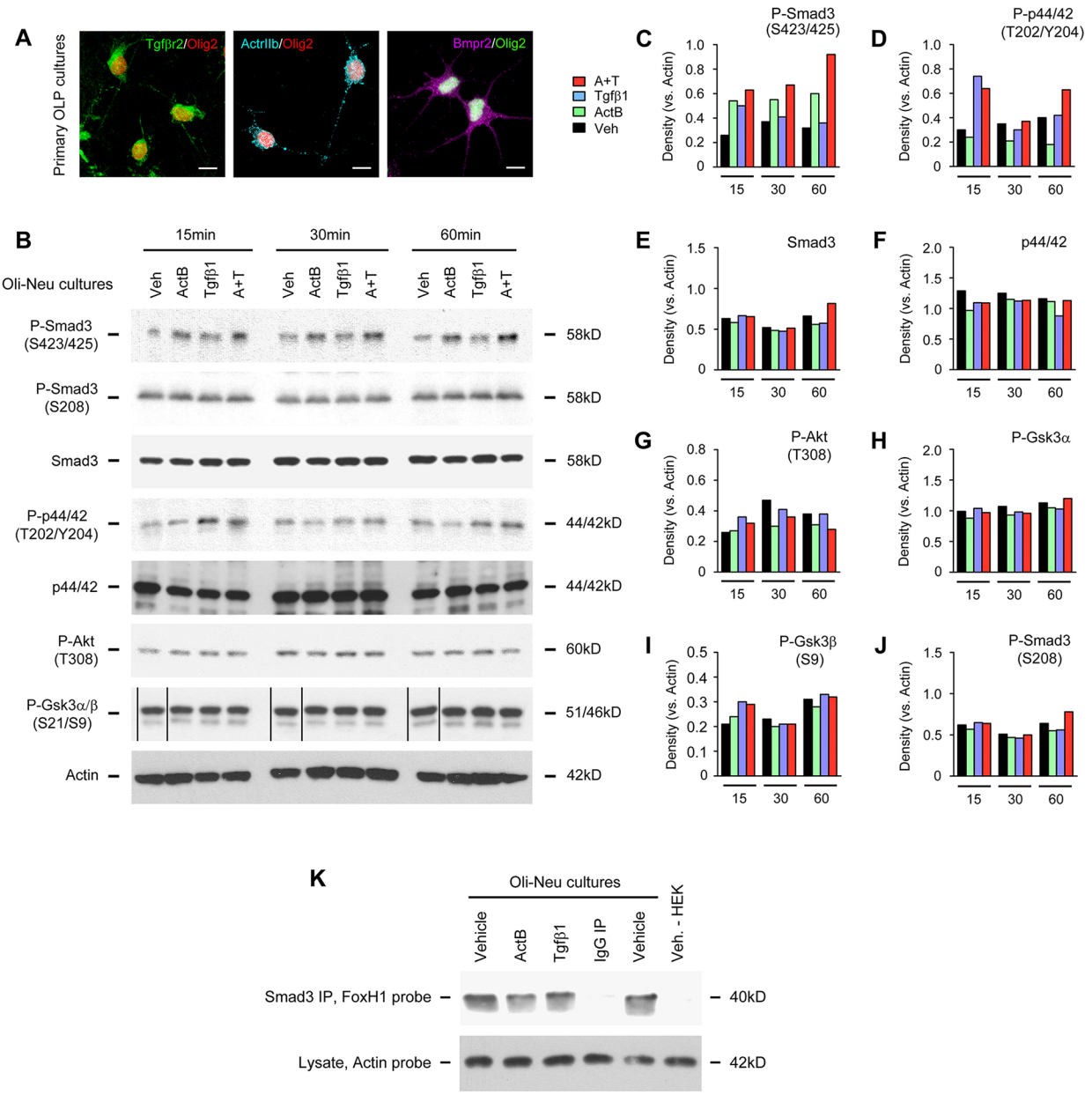

Fig. S3. Tgfβ1, ActB and co-treatment of Oli-Neu cells elicit distinct patterns of canonical Smad-dependent and non-canonical MAP kinase signaling. (A) Primary rat OLP cultures grown in medium favoring proliferation and non-permissive for differentiation were fixed, immunolabeled for Tgfβ superfamily ligand-binding receptors and Olig2, and imaged by confocal microscopy. Cells were ubiquitously positive for Tgfβr2, ActrIIb and Bmpr2. (B-J) Immunoblotting (B) and densitometric data (C-J) from Oli-Neu cells plated into serum-free media and exposed to 50ng/ml Tgfβ1 and/or ActB for 15, 30 or 60min. Findings complement data from primary OLP in Figs.3A and 3B. (B,C) Tgfβ1 or ActB alone each induced Smad3 phosphorylation at Ser423/425, although the effect of Tgfβ1 was lost by 60min. However, the effect of ActB was stronger than the equivalent Tgfβ1 concentration at all three timepoints, and this difference became more pronounced over time. In contrast, Tgfβ1 activation of p42/44 MAP kinase (P-Thr202/Tyr204) was seen at 15min, whereas ActB treatment persistently reduced p42/44 phosphorylation (B,D). Notably, co-treatment with Tgfβ1 plus ActB together produced a third distinct pattern, which combined increased levels of P-Smad3 (Ser423/425) similar to or beyond those induced by ActB alone, with increased phosphorylation of p42/44 MAP kinase beyond that induced by Tgfβ1 alone at later timepoints (B-D). No significant changes were seen in levels of total Smad3 or p42/44 proteins (B,E,F). Neither ligand alone or in combination impacted activity of the Akt-Gsk3 signaling pathway, as measured by changes in levels of phosphorylated Akt (P-Thr308) or Gsk3α/β (P-Ser21/9) (B,G-I). Smad3 phosphorylation within its linker region at Ser208 resulting from non-canonical pathway activation has been shown to alter its transcriptional activity, but no changes in Smad3 (P-Ser208) were detected in Tgfβ1- or ActB-treated cultures (B,J). (K,L) Oli-Neu cultures plated into serum-free media were exposed to 50ng/ml Tgfβ1, ActB or vehicle for 30min, then were subjected to co-immunoprecipitation using anti-Smad3 antibody or IgG control. HEK cells were used for comparison of cell type specificity. Immunoprecipitates and lysates were then subjected to immunoblotting and densitometric analysis. Blots of immunoprecipitates were probed for potential Smad3-interacting coactivators, and lysate blots were probed for actin (loading control). In Oli-Neu cells (but not HEK cells), Smad3 was found to associate with FoxH1/FAST (K), but not with other potential Smad-interacting factors, including ETF, Sp-1, Gli, TCF, or FoxO1. No differences in Smad3 binding to FoxH1/FAST were observed following ActB or Tgfβ1 treatment (K,L). Data are representative of findings from 3 independent experiments in separate cultures. Scale bars, 10 μm (A).

The authors apologise to the journal and readers for these errors.

© 2014. Published by The Company of Biologists Ltd | Development (2014) 141, 2414-2428 doi:10.1242/dev.106492

RESEARCH ARTICLE

STEM CELLS AND REGENERATION

Combinatorial actions of Tgfβ and Activin ligands promote oligodendrocyte development and CNS myelination

Dipankar J. Dutta[1,2,3], Andleeb Zameer[1,2,3], John N. Mariani[1,2,3], Jingya Zhang[1,2,3], Linnea Asp[1,2,3], Jimmy Huynh[2,3,4], Sean Mahase[1,2,3], Benjamin M. Laitman[1,2,3], Azeb Tadesse Argaw[1,2,3], Nesanet Mitiku[1,2,3], Mateusz Urbanski[5], Carmen V. Melendez-Vasquez[5], Patrizia Casaccia[2,3,4], Fernand Hayot[1,3,6], Erwin P. Bottinger[7,8], Chester W. Brown[9,10] and Gareth R. John[1,2,3,*]

ABSTRACT

In the embryonic CNS, development of myelin-forming oligodendrocytes is limited by bone morphogenetic proteins, which constitute one arm of the transforming growth factor-β (Tgfβ) family and signal canonically via Smads 1/5/8. Tgfβ ligands and Activins comprise the other arm and signal via Smads 2/3, but their roles in oligodendrocyte development are incompletely characterized. Here, we report that Tgfβ ligands and activin B (ActB) act in concert in the mammalian spinal cord to promote oligodendrocyte generation and myelination. In mouse neural tube, newly specified oligodendrocyte progenitors (OLPs) are first exposed to Tgfβ ligands in isolation, then later in combination with ActB during maturation. In primary OLP cultures, Tgfβ1 and ActB differentially activate canonical Smad3 and non-canonical MAP kinase signaling. Both ligands enhance viability, and Tgfβ1 promotes proliferation while ActB supports maturation. Importantly, co-treatment strongly activates both signaling pathways, producing an additive effect on viability and enhancing both proliferation and differentiation such that mature oligodendrocyte numbers are substantially increased. Co-treatment promotes myelination in OLP-neuron co-cultures, and maturing oligodendrocytes in spinal cord white matter display strong Smad3 and MAP kinase activation. In spinal cords of ActB-deficient *Inhbb*$^{-/-}$ embryos, apoptosis in the oligodendrocyte lineage is increased and OLP numbers transiently reduced, but numbers, maturation and myelination recover during the first postnatal week. *Smad3*$^{-/-}$ mice display a more severe phenotype, including diminished viability and proliferation, persistently reduced mature and immature cell numbers, and delayed myelination. Collectively, these findings suggest that, in mammalian spinal cord, Tgfβ ligands and ActB together support oligodendrocyte development and myelin formation.

KEY WORDS: Transforming growth factor, Activin, Smad, Oligodendrocyte, Myelin

[1]Neurology, Mount Sinai School of Medicine, New York, NY 10029, USA. [2]Corinne Goldsmith Dickinson Center for MS, Mount Sinai School of Medicine, New York, NY 10029, USA. [3]Friedman Brain Institute, Mount Sinai School of Medicine, New York, NY 10029, USA. [4]Neuroscience, Mount Sinai School of Medicine, New York, NY 10029, USA. [5]Biological Sciences, Hunter College, New York, NY 10065, USA. [6]Systems Biology, Mount Sinai School of Medicine, New York, NY 10029, USA. [7]Nephrology, Mount Sinai School of Medicine, New York, NY 10029, USA. [8]Charles Bronfman Institute for Personalized Medicine, Mount Sinai School of Medicine, New York, NY 10029, USA. [9]Molecular and Human Genetics, Baylor College of Medicine, Houston, TX 77030, USA. [10]Pediatrics, Baylor College of Medicine, Houston, TX 77030, USA.

*Author for correspondence (gareth.john@mssm.edu)

Received 27 November 2013; Accepted 15 April 2014

INTRODUCTION

Within CNS white matter, oligodendrocytes form myelin sheaths that facilitate efficient nerve impulse transmission (Li et al., 2009). Their origins have been studied in developing spinal cord, and oligodendrocyte progenitors (OLPs) are known to be produced in two phases (Richardson et al., 2006). The first occurs ventrally in the motor neuron progenitor (pMN) domain of periventricular neuroepithelium (Orentas and Miller, 1996) in response to sonic hedgehog induction of Olig transcription factors (Lu et al., 2000). The second phase is more dorsal (Cai et al., 2005) and depends on inhibition or downregulation of roof plate-derived bone morphogenetic proteins (Bmps), which restrict lineage specification and maturation (Mekki-Dauriac et al., 2002; Miller et al., 2004). Following specification, OLPs proliferate and migrate within the parenchyma, then differentiate into myelinating cells in white matter tracts (Fancy et al., 2011).

Bmps comprise one arm of the transforming growth factor-β (Tgfβ) family and signal canonically via R-Smads 1/5/8 (Munoz-Sanjuan and Brivanlou, 2002). The other arm includes Tgfβ1-5 and Activins, which signal via R-Smads 2/3 (Shi and Massague, 2003). Notably, the roles of this Smad2/3-activating cohort in oligodendrocyte development remain incompletely characterized. Complementary patterns of Tgfβ1-3 expression have been reported in embryonic mouse spinal cord (Flanders et al., 1991; Mecha et al., 2008), and Tgfβ1 has been shown to regulate Pdgf-driven proliferation of O-2A cells *in vitro* (McKinnon et al., 1993), while interactions between Olig2 and Smad3 have been linked to boundary determination of the pMN domain at HH stages 12-18 in chick neural tube (Garcia-Campmany and Marti, 2007; Estaras et al., 2012). Studies have also reported expression of activin B (ActB) subunit and ActrIIb receptor mRNAs in developing mouse CNS at stages including those of OLP generation (Feijen et al., 1994). These findings are further compatible with known roles of Activins as regulators of neuronal survival and differentiation (Schubert et al., 1990; Poulsen et al., 1994; Krieglstein et al., 1995; Cambray et al., 2012).

Here, we report that, in contrast to Bmp signaling, Tgfβ ligands and ActB act in combination in the developing mammalian spinal cord to promote oligodendrocyte development and myelination. Our expression analyses in mouse embryos indicate that, following lineage specification, OLPs are exposed to Tgfβ ligands first alone, then in combination with ActB during maturation. In isolation, Tgfβ ligands and ActB differentially activate canonical Smad3 and non-canonical MAP kinase signaling. Both enhance viability, and Tgfβ ligands promote proliferation whereas ActB enhances differentiation. In combination, they strongly activate both signaling pathways. Together, their impact on viability is additive, and proliferation and differentiation are both enhanced, resulting in a substantial increase in mature oligodendrocyte numbers. In ActB-deficient *Inhbb*$^{-/-}$ mouse embryos, apoptosis is increased within the lineage, and OLP numbers are transiently reduced.

Development (2014) 141, 2414-2428 doi:10.1242/dev.106492

Notably, *Smad3*$^{-/-}$ embryos display more severe defects in viability, mitosis and maturation, and these result in delayed myelination.

RESULTS

Localization of Smad3 activity in E12.5 mouse spinal cord

We analyzed embryonic mouse spinal cord for patterns of canonical Smad2/3 activity, and correlated these with expression profiles of Tgfβ and Activin ligands (Figs 1 and 2; supplementary material Fig. S1). Notably, these immunohistochemical studies revealed phosphorylated (active) Smad3, but not Smad2, in oligodendrocyte lineage cells from embryonic day (E) 12.5, shortly after ventral OLP specification (Fig. 1; supplementary material Fig. S1). At E12.5, Smad3 protein and phospho-Smad3 (P-Ser423/425) were detected in cell nuclei throughout the periventricular neuroepithelium (Fig. 1A-C), including Olig2^{+} OLPs in the pMN domain (Fig. 1A; supplementary material Fig. S1A). Total and phospho-Smad3 also localized to Lim1^{+} Dl1/Dl2 neurons dorsolaterally in the parenchyma, and to the floor plate ventrally (Fig. 1A; supplementary material Fig. S1A,B). No immunoreactivity was detected in *Smad3*$^{-/-}$ embryos (negative control). These findings were similar, but not identical, to previous reports in chick, in which Smad3 is expressed in periventricular neuroepithelium but is relatively low in the pMN domain at the equivalent stage (Garcia-Campmany and Marti, 2007; Estaras et al., 2012). Compatible with previous findings, Smad2 was not detected (Garcia-Campmany and Marti, 2007). Reports differ as to the extent of Smad2 expression in the neural tube during embryogenesis (Garcia-Campmany and Marti, 2007; Miguez et al., 2013).

Differential patterns of Tgfβ and Activin ligands in mouse spinal cord at E12.5

Further analyses suggested that in developing spinal cord, Smad3 activity might first result from exposure to Tgfβ1-3 in periventricular neuroepithelium, then to these and ActB together in the

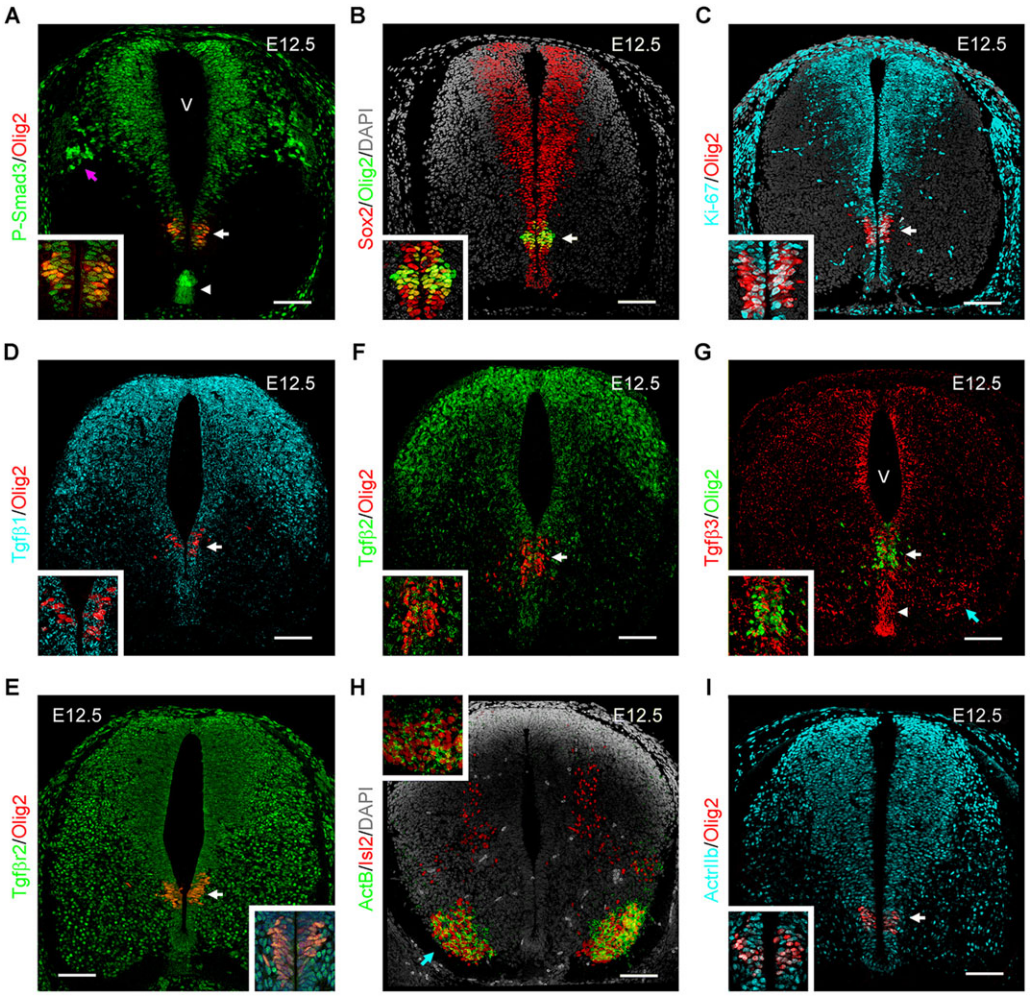

Fig. 1. Smad3 activation in E12.5 mouse spinal cord. Spinal cord sections from E12.5 C57BL/6 embryos immunolabeled for Smad3 and Tgfβ and Activin ligands and receptors. (A-C) Phospho-Smad3 (P-Ser423/425) was detected throughout the Sox2^{+} periventricular neuroepithelium (A,B), which is proliferating (Ki67^{+}) (C). See also supplementary material Fig. S1A. Olig2^{+} OLPs in the pMN domain were P-Smad3^{+} (A, white arrow and inset). P-Smad3 also localized to Lim1^{+} Dl1/Dl2 neurons dorsolaterally (magenta arrow; see supplementary material Fig. S1A,B) and to the floor plate (arrowhead). V, ventricle. (D-G) Expression of Tgfβ1-3 and Tgfβr2. Olig2^{+} cells are arrowed and magnified in the inset. Similar to P-Smad3, Tgfβ1 localized extracellularly to Sox2^{+} periventricular neuroepithelium including the pMN domain, and to Lim1^{+} neurons dorsolaterally (D). See also supplementary material Fig. S1B. Tgfβr2 localized to cells throughout the spinal cord, including Olig2^{+} OLPs (E). Tgfβ2 displayed a similar distribution to Tgfβ1 (F), whereas Tgfβ3 localized extracellularly to ventral periventricular zone and floorplate (G, arrowhead), and to the ventrolateral motor neuron domain (blue arrow). (H,I) Distribution of ActB and ActrIIb. ActB was detected extracellularly within the Mnr^{+} Isl2^{+} ventrolateral motor neuron domain (H, blue arrow and inset). See also supplementary material Fig. S1C,D. ActrIIb was expressed by cells throughout the periventricular neuroepithelium and dorsolateral cord, including Olig2^{+} OLPs (I, arrow and inset). Data are representative of samples from at least four individuals. Scale bars: 50 µm.

Development (2014) 141, 2414-2428 doi:10.1242/dev.106492

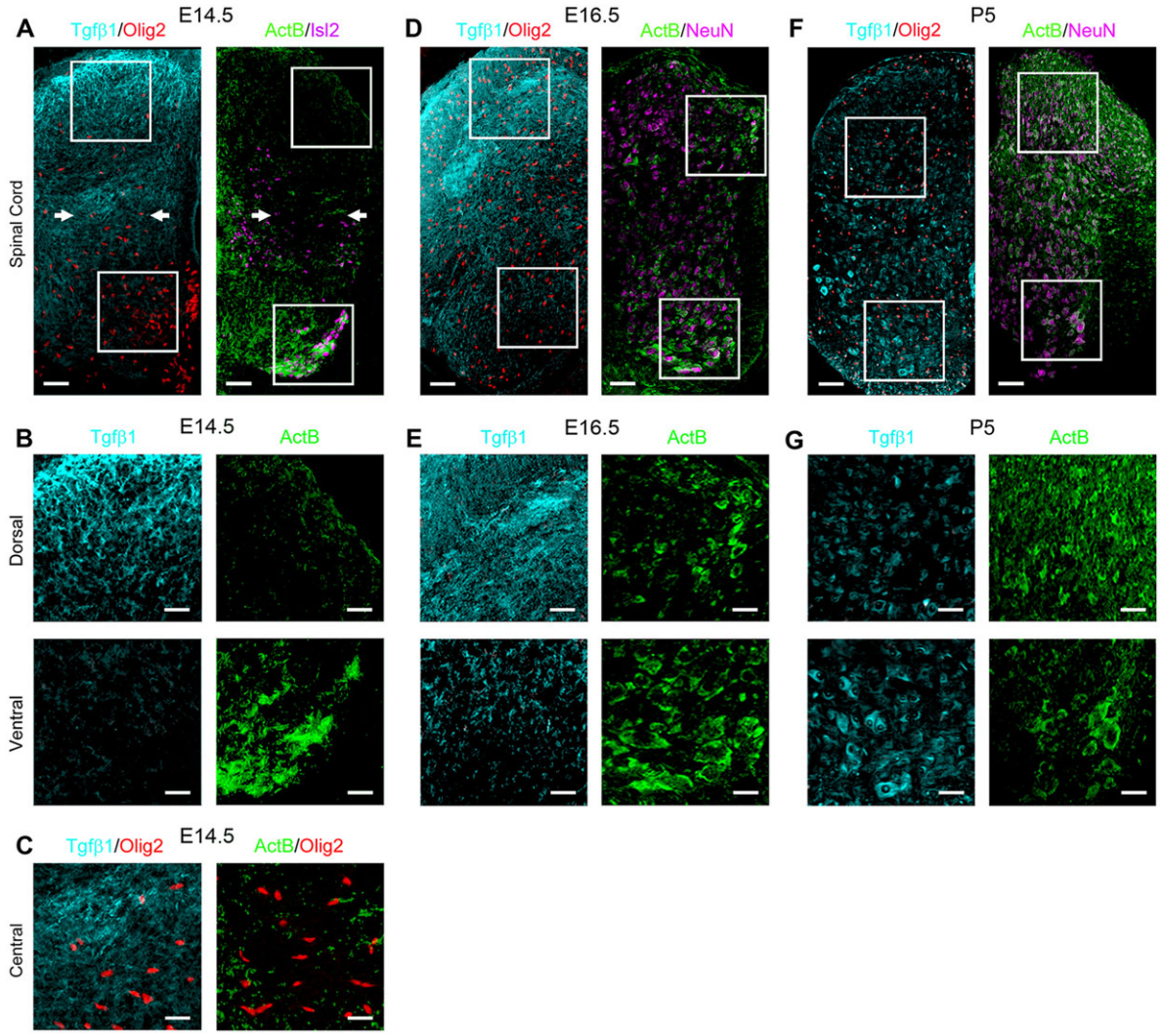

Fig. 2. Progressive overlap of Tgfβ1 and ActB during spinal cord development. (A,D,F) C57BL/6 spinal cords at E14.5, E16.5 and P5. In each, the left panel shows half a spinal cord immunolabeled for Tgfβ1 and Olig2, whereas the right panel illustrates immunoreactivity for ActB and Isl2 or NeuN. Representative (boxed) dorsal and ventral areas are shown at higher magnification in B,E,G. The central zone in A (arrowed) is shown at higher magnification in C in the case of Tgfβ1/Olig2 (left panel). The right panel in C shows ActB/Olig2 staining in the same area from an immediately adjacent section. By E14.5, Tgfβ1 expression began to expand ventrally within the parenchyma, such that it began to overlap with Olig2^{+} cells outside the periventricular neuroepithelium (A-C). Ventral spread continued during later embryogenesis (E16.5; D,E), and postnatally. By P5, when the spinal cord is myelinating, Tgfβ1 localized to neurons throughout the cord (F,G). Concurrently, ActB expression spread dorsally and medially. At E14.5, the pattern of ActB overlapped minimally with Olig2^{+} cells (A-C). By E16.5, ActB localized more widely throughout the parenchyma (D,E), and by P5 neuronal expression was widespread (F,G). Data are representative of four individuals at each time point. Scale bars: 70 µm in A; 15 µm in B,C; 150 µm in D; 30 µm in E; 250 µm in F; 60 µm in G.

parenchyma. Tgfβ1 has highest affinity for the ligand-binding Tgfβr2 receptor (Shi and Massague, 2003) and, compatible with Smad3 activity and a previous report (Mecha et al., 2008), at E12.5 Tgfβ1 protein localized extracellularly throughout periventricular neuroepithelium, and to the Lim1^{+} neuronal domain (Fig. 1D; supplementary material Fig. S1B). Tgfβr2 localized to cells throughout the spinal cord, including Olig2^{+} OLPs (Fig. 1E). We also detected the lower affinity ligands Tgfβ2 and Tgfβ3, with the former localizing extracellularly to the periventricular neuroepithelium and dorsolaterally (Fig. 1F), and the latter to the ventral periventricular zone and floorplate and the ventrolateral motor neuron domain (Fig. 1G). Thus, at E12.5 Olig2^{+} OLPs were exposed to Tgfβ1-3, expressed Tgfβr2, and were positive for Smad3 activity.

By contrast, at E12.5 ActB localized extracellularly to the Mnr^{+} Isl2^{+} ventrolateral motor neuron domain in the parenchyma (Fig. 1H; supplementary material Fig. S1C,D). Activins A, B and AB are dimers of Inhβa and Inhβb, and *in situ* hybridization for *Inhbb* produced identical findings (supplementary material Fig. S1C,D). Samples from *Inhbb*$^{-/-}$ embryos produced no signal. The ligand-binding receptor ActrIIb localized throughout the periventricular neuroepithelium and dorsolateral cord (Fig. 1I), in agreement with a previous report (Feijen et al., 1994). We did not detect ActrIIb localization to the Mnr^{+} Isl2^{+} domains, the sites of ActB expression (Fig. 1I). Compatible with previous findings, ActA and *Inhba* were not detected (Feijen et al., 1994).

These data suggested that Tgfβ ligands are a significant source of Smad3 activity at E12.5 throughout the periventricular neuroepithelium, including Olig2^{+} OLPs. Although these cells also expressed ActrIIb, at E12.5 the source of ActB lay outside the periventricular zone, in the ventrolateral Mnr^{+} Isl2^{+} domain.

Development (2014) 141, 2414-2428 doi:10.1242/dev.106492

Progressive overlap of Tgfβ1 and ActB during spinal cord development

Notably, these patterns subsequently changed, reflecting progressive overlap of Tgfβ and ActB signaling (Fig. 2; supplementary material Figs S1 and S2). This was detectable by E14.5, at which time OLPs expand into the parenchyma (Cai et al., 2005; Fogarty et al., 2005; Zhang et al., 2006). Coincident with this expansion, the distribution of Tgfβ1 spread ventrally, such that it began to overlap with Olig2$^+$ cells outside the periventricular neuroepithelium (Fig. 2A-C). The distribution of Tgfβ2 also expanded ventrally (supplementary material Fig. S1E), but Tgfβ3 remained confined to the periventricular zone, floorplate and ventrolateral parenchyma (supplementary material Fig. S1F). Ventral spread of Tgfβ1 continued during later embryogenesis (E16.5, Fig. 2D,E) and postnatally. By postnatal day (P) 5, when the spinal cord is myelinating, Tgfβ1 localized to neurons throughout the cord (Fig. 2F,G).

Concurrent with this increase in the distribution of Tgfβ ligands, ActB also spread dorsally and medially, albeit lagging behind the dorsal expansion of OLPs at E14.5 (Fig. 2A-C). By E16.5, ActB localization encompassed neuronal domains centrally and dorsally (Fig. 2D,E), and this trend continued until, by P5, neuronal expression was widespread (Fig. 2F,G). Thus, by the onset of myelination, Tgfβ1 and ActB overlapped almost completely.

Indicating that the oligodendrocyte lineage remained sensitive to Tgfβ and Activin ligands postnatally, at P5 both Tgfβr2 and ActrIIb localized to Olig2$^+$ cells, including Pdgfrα$^+$ OLPs and mature CC-1$^+$ oligodendrocytes, as well as to other lineages, including NeuN$^+$ neurons (supplementary material Fig. S2A-F).

Together, these data suggested that OLPs in the developing spinal cord are initially exposed to Tgfβ ligands, then to these and ActB together. This suggested the potential for complementary functions and additive or synergistic outcomes.

Distinct signaling profiles produced by Tgfβ1, ActB, and co-treatment in OLPs *in vitro*

We compared the impact of Tgfβ1 and ActB individually and in combination in primary OLPs and the oligodendrocyte-derived Oli-Neu cell line (Figs 3 and 4; supplementary material Figs S3 and S4). Immunocytochemistry confirmed ubiquitous Tgfβr2 and ActrIIb expression in OLPs (supplementary material Fig. S3A) and Oli-Neu cells (not shown). Initially, we evaluated the activation of canonical and non-canonical signaling in response to 1-100 ng/ml Tgfβ1, ActB, and co-treatment, in timecourse studies in Oli-Neu cells (supplementary material Fig. S3B-K), validated in primary OLPs (Fig. 3A,B). Although Act/Tgfβ ligands canonically activate Smad2/3, they also signal non-canonically via the p38/Erk/Jnk MAP kinase and PI3 kinase-Akt-Gsk3 pathways (Massague, 2012). Notably, examination of Smad3 and MAP kinase and Akt-Gsk3 activation profiles revealed that Tgfβ1 and ActB produced different patterns of canonical and non-canonical signaling, and that, crucially, in combination they elicited a third distinct response.

In both sets of cultures, Tgfβ1 and ActB both induced Smad3 phosphorylation at Ser423/425, but ActB produced a stronger, more prolonged effect than the same Tgfβ1 concentration (supplementary material Fig. S3B,C; Fig. 3A,B). ActB also reduced activation (phosphorylation) of p38 (P-Thr180/Tyr182) and p42/44 (P-Thr202/Tyr204) MAP kinases, which has been linked to reinforcement of Smad activation (Kretzschmar et al., 1999; Grimm and Gurdon, 2002). By contrast, Tgfβ1 briefly increased MAP kinase activation (supplementary material Fig. S3B,D; Fig. 3A,B). Importantly, co-treatment with ActB plus Tgfβ1 produced levels of phospho-Smad3 similar to, or greater than, ActB alone, and increased p38 and p42/44 phosphorylation beyond Tgfβ1 alone at later time points (30-60 min) (supplementary material Fig. S3B-D; Fig. 3A,B). Total Smad3 and MAP kinase protein levels were unaltered (supplementary material Fig. S3B,E,F). No activation of c-Jun (P-Ser63/73) was detected (data not shown). Neither ligand alone, nor in combination, impacted Akt (P-Thr308) or Gsk3α/β (P-Ser21/9) activity (supplementary material Fig. S3B,G-I).

Analysis of other regulatory mechanisms reported as Tgfβ1/ActB-sensitive in other cell types revealed no further differential outcomes. Smad3 phosphorylation within its linker region at Ser208 has been shown to alter its transcriptional activity (Kretzschmar et al., 1999; Funaba et al., 2002), but we detected no changes in Smad3 (P-Ser208) activity (supplementary material Fig. S3B,J). Additionally, we used co-immunoprecipitation to examine Smad3 interactions with potential co-activators, with Foxh1 serving as a positive control (Chen et al., 1996; Attisano et al., 2001). However, although we detected Smad3 association with Foxh1, we did not detect interactions with other co-activators, including ETF (Tead2), Sp1, Gli, TCF (Hnf4a) and Foxo1, nor any differential Smad3 binding to Foxh1 upon ActB or Tgfβ1 treatment (supplementary material Fig. S3K,L).

Interestingly, Tgfβ1 and ActB signaling were subject to regulation by Bmp. OLPs expressed Bmpr2 (supplementary material Fig. S3A), and, in agreement with previous work (De Robertis and Kuroda, 2004), in OLP cultures Bmp4 dose-dependently induced phosphorylation of Smads 1/5 (P-Ser463/465) but not Smad3 or MAP kinases (Fig. 3A,B; supplementary material Fig. S4A-D). However, Bmp4 dose-dependently abrogated ActB- or Tgfβ1-induced Smad3 phosphorylation, but ActB or Tgfβ1 was unable to inhibit Bmp4 Smad1/5 activation (supplementary material Fig. S4A-D).

Co-treatment of OLPs with Tgfβ1 and ActB elicits combinatorial functional outcomes

These data indicated that exposure of OLPs to Tgfβ ligands in isolation versus in combination with ActB produced differential signaling profiles. Importantly, further analyses confirmed that these correlated with distinct functional outcomes (Fig. 3C-J; supplementary material Fig. S4E-G). In primary OLP cultures grown for 5 days in serum-free media, proliferating OLPs exit the cell cycle and mature into Cnp$^+$ Mbp$^+$ oligodendrocytes (Zhang et al., 2011). Initial immunoblotting studies revealed that treatment of cultures with Tgfβ1 or ActB alone or in combination reduced caspase-3 cleavage (reflecting apoptotic activity), and that ActB or co-treatment also enhanced maturation marker expression (Fig. 3C,D). In more comprehensive morphometric timecourse studies, both Tgfβ1 and ActB reduced the number and fraction of apoptotic cells (Fig. 3E,F; supplementary material Fig. S4E). In addition, Tgfβ1 increased numbers of Olig2$^+$ oligodendrocyte lineage cells, and the number and fraction of proliferating BrdU-labeled Olig2$^+$ cells, and of immature cells expressing Olig2 but not maturation markers (Fig. 3G-I; supplementary material Fig. S4F). By contrast, ActB increased the number and fraction of mature Mbp$^+$ oligodendrocytes (Fig. 3J; supplementary material Fig. S4G). Crucially, co-treatment produced a combination of these outcomes. Co-treatment reduced apoptosis more strongly than Tgfβ1 or ActB, and increased Olig2$^+$ and BrdU$^+$ Olig2$^+$ cells similar to Tgfβ1 alone (Fig. 3F-H; supplementary material Fig. S4E,F). Importantly, co-treatment also strongly potentiated the impact of ActB on mature cell number. In co-treated cultures, the fraction of Mbp$^+$ cells was similar to that in ActB-treated cultures (supplementary material Fig. S4G), but the overall Olig2$^+$ population was significantly larger (Fig. 3H); thus, the total increase in Mbp$^+$ cells was almost double that seen in cultures treated with ActB alone (Fig. 3J). Different markers for

Development (2014) 141, 2414-2428 doi:10.1242/dev.106492

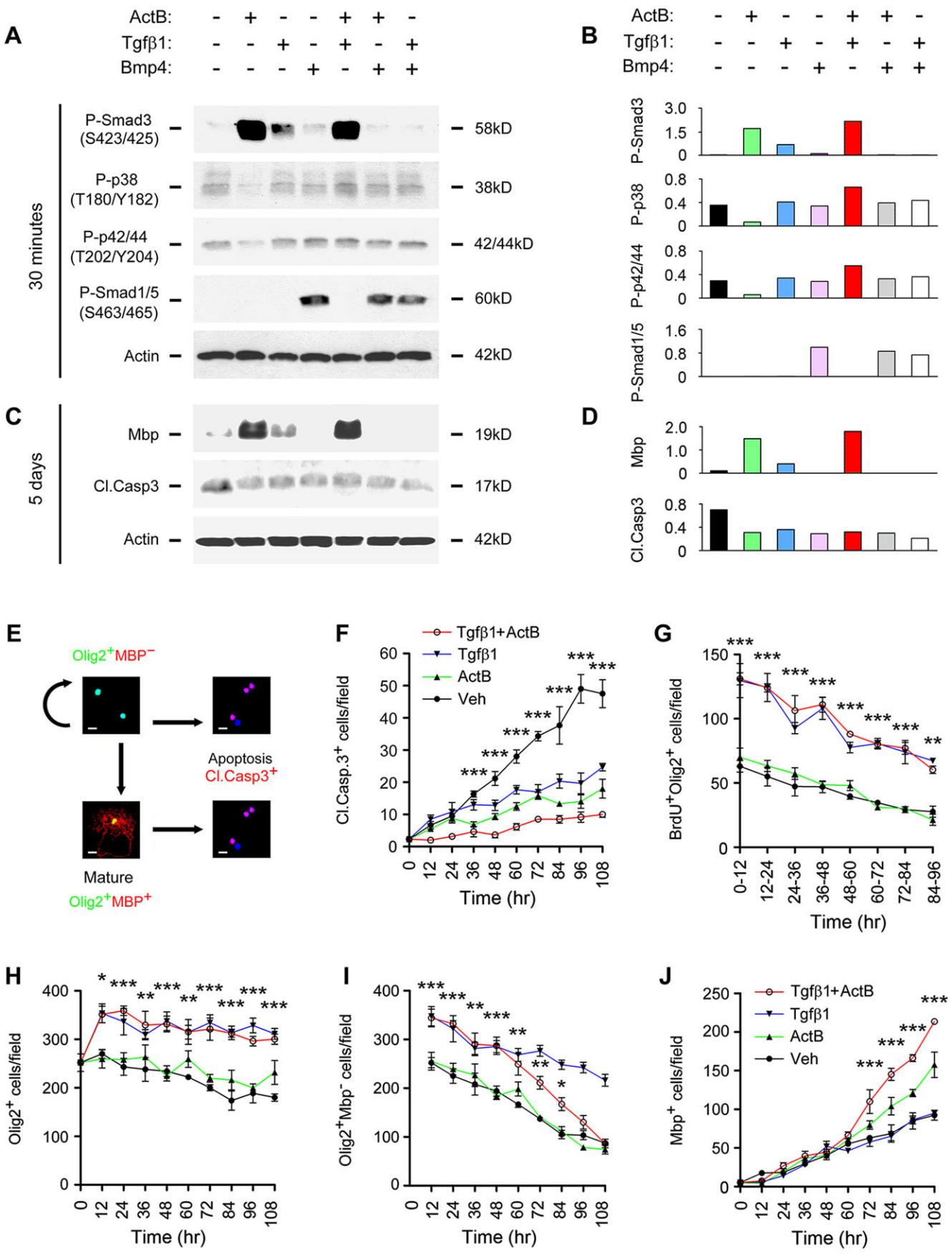

Fig. 3. See next page for legend.

Development (2014) 141, 2414-2428 doi:10.1242/dev.106492

Fig. 3. Tgfβ1, ActB and co-treatment elicit distinct signaling and functional outcomes in OLPs. (A-D) Immunoblotting (A,C) and densitometry (B,D) of primary OLPs plated into serum-free media and exposed to 50 ng/ml Tgfβ1, ActB and/or Bmp4 for 30 min (A,B) or 5 days (C,D). (A,B) Results complement signaling timecourse data from Oli-Neu cells (supplementary material Fig. S3A-L) and from OLPs (supplementary material Fig. S4A-D). (C,D) Data accompany morphometric timecourse analyses in OLPs in E-J and supplementary material Fig. S4E-G. (A,B) In OLPs, Tgfβ1 and ActB both induced Smad3 phosphorylation (P-Ser423/425), but ActB produced stronger stimulation than the equivalent Tgfβ1 concentration. ActB also reduced phosphorylation of p38 (P-Thr180/Tyr182) and p42/44 (P-Thr202/Tyr204). Co-treatment produced Smad3 phosphorylation similar to, or greater than, ActB alone, without inhibition of MAP kinase phosphorylation; rather, co-treatment increased phospho-p38 (P-Thr180/Tyr182) and p42/44 (P-Thr202/Tyr204). See also supplementary material Fig. S3A-F. Conversely, Bmp4 induced phosphorylation of Smads 1/5 (P-Ser463/465) but not Smad3. Co-treatment with Tgfβ1 or ActB plus Bmp4 abrogated Smad3 phosphorylation but not Smad1/5/8 phosphorylation. See also supplementary material Fig. S4A-D. (C,D) At 5 days, caspase-3 cleavage (a marker of apoptotic activity) was decreased in OLP cultures exposed to Tgfβ or ActB alone or together. Mbp expression (mature oligodendrocytes) was enhanced in ActB-treated and co-treated cultures. Bmp alone or in combination with Tgfβ or ActB abrogated Mbp expression. (E-J) OLPs grown in serum-free media and treated with 50 ng/ml Tgfβ1, ActB or both were harvested at 12 h intervals for up to 5 days and stained for Olig2, Mbp, cleaved caspase-3 and BrdU labeling (proliferation) (E). Data are presented as raw cell counts. The same results are presented as fractions of total $Olig2^+$ cells in supplementary material Fig. S4E-G. In controls, mature Mbp^+ cells progressively increased, proliferating progenitors decreased, and apoptosis gradually increased. Tgfβ1 or ActB reduced numbers of apoptotic cells (F). Tgfβ1 also amplified numbers of proliferating $BrdU^+$ $Olig2^+$, total $Olig2^+$ and immature $Olig2^+$ Mbp^- cells (G-I), whereas ActB increased mature Mbp^+ oligodendrocytes (J). Co-treatment reduced apoptotic cell number more substantially than either ligand alone, and increased $BrdU^+$ $Olig2^+$ and total $Olig2^+$ cells similar to Tgfβ1 (F-H). Co-treatment also potentiated the impact of ActB on mature Mbp^+ oligodendrocyte number. In co-treated cultures, the fraction of Mbp^+ cells was similar to that in ActB-treated cultures (see supplementary material Fig. S4G), but the $Olig2^+$ population was larger, and thus Mbp^+ cell number was strongly augmented (J). Data are representative of three studies in separate cultures. (F-J) Two-way ANOVA plus Bonferroni post-test; $^*P<0.05$, $^{**}P<0.01$, $^{***}P<0.001$, for co-treated versus vehicle (Veh) control cultures. Error bars indicate s.e.m.

immature versus mature cells (OLP, Pdgfrα; oligodendrocyte, Plp) produced identical findings.

Tgfβ1 and ActB synergistically promote oligodendrocyte maturation and enhance viability

To validate these outcomes, from morphometric data we used a previously described mathematical model to calculate coefficients for proliferation in the $Olig2^+$ Mbp^- (OLP plus immature oligodendrocyte) versus $Olig2^+$ Mbp^+ (mature) populations (α, γ), differentiation from one to the other (β), and net apoptosis (δ+ε) (Zhang et al., 2011; Hsieh et al., 2004) (Fig. 4A). Coefficients thus generated take into account rate of change of the measured parameters and population size. ActB and Tgfβ1 each reduced the coefficient of apoptosis (Fig. 4B), and Tgfβ1 increased the coefficient of proliferation (Fig. 4C), whereas ActB enhanced the coefficient of differentiation (Fig. 4D). All values for γ were zero, confirming the postmitotic status of Mbp^+ cells (not shown). Importantly, co-treatment produced a further reduction in the apoptosis coefficient (Fig. 4B), combined with strong enhancement of the differentiation coefficient (Fig. 4D).

Strong Smad3 and MAP kinase activity in differentiating oligodendrocytes in myelinating white matter

To test whether these *in vitro* profiles were also reflected *in vivo*, we returned to analyses of developing spinal cord (Fig. 5). OLPs *in vivo* are exposed to Tgfβ ligands first in isolation, and then in combination with ActB during maturation. Thus, we hypothesized that Smad3 and MAP kinase activity would be detectable in OLPs following specification and during expansion, and then increase in differentiating cells. A similar pattern has been described for Erk signaling in chick, with activity most pronounced in differentiating white matter (Kato et al., 2005). To test the hypothesis, we measured pixel intensity for Smad3 (P-Ser423/425) and p42/44 (P-Thr202/Tyr204) in cells positive for lineage or maturation markers at E12.5, during expansion at E14.5, and at the onset of myelination at P5. Smad3 activity could be assumed to result from Tgfβ/Activin signaling. MAP kinase pathways have been discussed in the context of OLP development (Schwammenthal et al., 2004; Fragoso et al., 2007; Fyffe-Maricich et al., 2011), and are also activated by factors beyond the Tgfβ family (Bhat and Zhang, 1996; Althaus et al., 1997; Yim et al., 2001).

Quantitative analysis confirmed detectable Smad3 (P-Ser423/425) activity in OLPs in the pMN domain at E14.5, as at E12.5 (Fig. 5A,B; compare with Fig. 1A). Activity was also detectable in $Olig2^+$ cells migrating into the parenchyma at E14.5, albeit at lower levels (Fig. 5A,B), consistent with the lower Tgfβ1 and Tgfβ2 activity in these areas at this time (compare with Fig. 2A). Notably, however, by P5 we observed a differential in Smad3 activity (Fig. 5B,C), which was high in $Olig2^+$ cells in maturing white matter and lower in $Olig2^+$ cells in gray matter (Fig. 5B,C). Further supporting our hypothesis, cells positive for maturation markers (CC-1) also displayed high-level activity in P5 white matter tracts (Fig. 5C).

Similar results were also observed for p42/44 activity, which in addition were similar to those reported in chick (Kato et al., 2005). At E12.5, p42/44 (P-Thr202/Tyr204) localized to cells in the ventral periventricular neuroepithelium, including OLPs (Fig. 5D,E), and to radial processes between this region and the pial surface (Fig. 5E). A similar pattern was seen at E14.5 (Fig. 5D,F), and levels of p42/44 activity in $Olig2^+$ cells in the pMN domain resembled those at E12.5 (Fig. 5D-F). Conversely, activity was detectable but low in $Olig2^+$ cells in the parenchyma at E14.5 (Fig. 5D,F). By P5, p42/44 (P-Thr202/Tyr204) localized predominantly to white matter, and to neurons within the dorsal horns (Fig. 5G). Activity was high in $Olig2^+$ cells and $CC\text{-}1^+$ cells in white matter tracts (Fig. 5D,G).

Together, these data suggested that the signaling profiles detected in response to Tgfβ1 and ActB treatment of OLPs *in vitro* are also reflected in the developing spinal cord, and are functionally relevant in the context of oligodendrocyte development. Consistent with our hypothesis, Smad3 and MAP kinase activity were both high in differentiating cells in white matter at P5, at the onset of myelination.

Co-treatment with Tgfβ1 plus ActB enhances myelin formation in OLP-neuron co-cultures

To investigate roles in myelin formation, we initially examined co-cultures of primary OLP and dorsal root ganglion (DRG) neurons (Fig. 6; supplementary material Fig. S5) (Chan et al., 2004). Co-cultures were left to myelinate in the presence of 50 ng/ml Tgfβ1, ActB, or both for 14 days, then stained for Olig2, Mbp and neurofilament (Nf, axons) and analyzed by morphometry. We also examined the impact of co-treatment with Bmp4, which studies in OLPs confirmed as a potent inhibitor of maturation (supplementary material Fig. S5A-D) (See et al., 2004).

Importantly, these experiments showed that myelination was enhanced by ActB and further increased by Tgfβ1 plus ActB co-treatment. At 14 days, controls and ActB-treated or Tgfβ1-treated co-cultures contained Mbp^+ oligodendrocytes, which

Development (2014) 141, 2414-2428 doi:10.1242/dev.106492

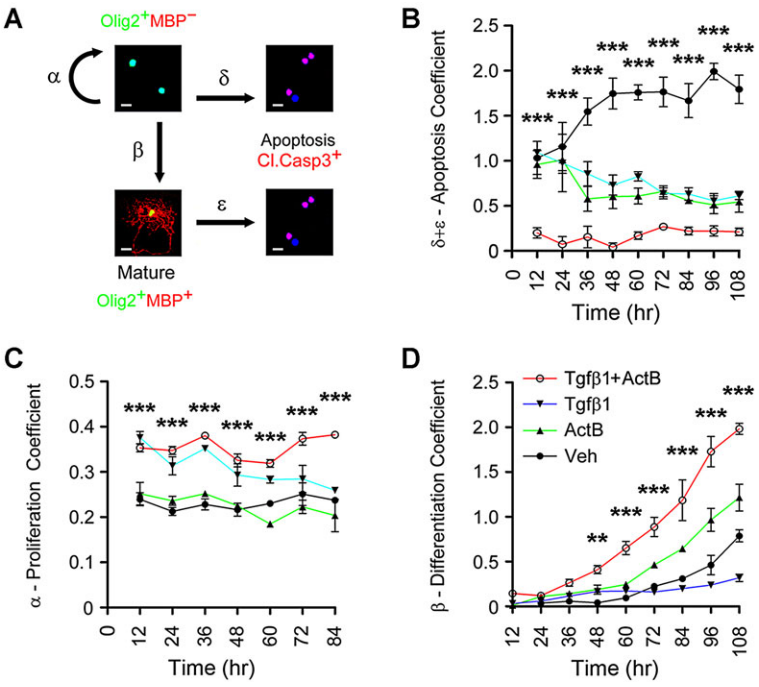

Fig. 4. Tgfβ1 and ActB synergistically promote oligodendrocyte maturation and enhance viability. Mathematical modeling analysis of morphometric data in Fig. 3F-J, to generate coefficients for proliferation within the Olig2$^+$ Mbp$^-$ (OLP plus immature oligodendrocyte) versus Olig2$^+$ Mbp$^+$ (mature oligodendrocyte) populations (α, γ), differentiation from one to the other (β), and net apoptosis within the culture (δ+ε) (as outlined in A and see Materials and Methods) (Zhang et al., 2011; Hsieh et al., 2004). Coefficients thus generated take into account rate of change of the measured parameters, and the size of the population. Both ActB and Tgfβ1 reduced the coefficient of apoptosis (B). Additionally, Tgfβ1 increased the coefficient of proliferation (C), whereas ActB enhanced the coefficient of differentiation (D). Importantly, co-treatment validated a further reduction in the coefficient of apoptosis (B), combined with strong enhancement of the coefficient of differentiation (D). Data are representative of findings from three independent experiments in separate cultures. (B-D) Two-way ANOVA plus Bonferroni post-test; **P<0.01, ***P<0.001, for co-treated versus control cultures. Error bars indicate s.e.m.

extended processes that co-localized with Nf$^+$ axons to form linear Mbp$^+$ Nf$^+$ profiles corresponding to compact myelin segments (Fig. 6A,B), as confirmed by electron microscopy (Fig. 6C). Co-cultures exposed to ActB contained more Mbp$^+$ cells and myelin segments than controls (Fig. 6D,E). Tgfβ1 alone did not enhance myelination, but, importantly, Tgfβ1 plus ActB co-treatment resulted in a further increase in Mbp$^+$ cells and segment numbers (Fig. 6A,D,E), also accompanied by an increase in myelination per Mbp$^+$ cell (Fig. 6F). By contrast, co-cultures exposed to Bmp4 contained almost no Mbp$^+$ cells or myelin segments, even in the presence of ActB co-treatment (Fig. 6D,E,G).

Transient impairment of oligodendrocyte development in ActB-deficient *Inhbb*$^{-/-}$ spinal cord

To investigate functional significance *in vivo*, we examined oligodendrocyte development and myelination in spinal cords of ActB-deficient *Inhbb*$^{-/-}$ and Smad3-deficient *Smad3*$^{ex8/ex8}$(*Smad3*$^{-/-}$) mice (Vassalli et al., 1994; Yang et al., 1999) (Figs 7 and 8; supplementary material Fig. S6). Constitutive models were preferred since they allowed inference of wider trends within the cord. These studies revealed that oligodendrocyte development was abnormal in both models, but that the phenotype of *Smad3*$^{-/-}$ mice was the more severe.

In *Inhbb*$^{-/-}$ embryos, oligodendrocyte development was transiently impaired, but recovered postnatally and myelination was not impacted (Fig. 7). At E12.5, differences in Olig2$^+$ cells did not reach significance (Fig. 7A,B). However, Olig2$^+$ numbers were reduced in *Inhbb*$^{-/-}$ embryos at E15.5, a time when their distribution begins to overlap with that of ActB (Fig. 7C,D). At E15.5, Olig2$^+$ Sox2$^-$ Sox9$^+$ progenitors are found in the parenchyma, and early-stage Olig2$^+$ Sox2$^+$ progenitors remain in the periventricular zone (Stolt et al., 2003). In *Inhbb*$^{-/-}$ embryos, the former were decreased, but no changes were detected in the latter (Fig. 7C,D). We hypothesized that the former population might be more sensitive to changes in ActB support. Cleaved caspase-3$^+$ Olig2$^+$ apoptotic cells were increased in E15.5 *Inhbb*$^{-/-}$ samples (Fig. 7E), but cycling Ki67$^+$ Olig2$^+$ cells were unaltered (Fig. 7F).

Interestingly, this phenotype self-corrected postnatally. Multiple pathways contribute to the generation of myelinating cells, and a strong precedent exists for recovery of myelination in mutants showing deficits in progenitor development (Montag et al., 1994; Larsen et al., 2006; Lewallen et al., 2011). Postnatally in *Inhbb*$^{-/-}$ spinal cords, the fraction of apoptotic Olig2$^+$ cells remained slightly but significantly increased, and the fraction of cycling Ki67$^+$ Olig2$^+$ cells was marginally (but significantly) raised (Fig. 7E,F), but by P5 the numbers of Olig2$^+$ cells in *Inhbb*$^{-/-}$ and control cords were similar (Fig. 7G-I). No significant differences were detected in the numbers of Olig2$^+$ Pdgfrα$^+$ OLPs or in more mature CC-1$^+$ oligodendrocytes (Fig. 7G). Cells expressing the early myelin protein Mag (myelin-associated glycoprotein) were reduced, but immunoreactivity for other myelin proteins was normal (Fig. 7G-I).

These findings suggested that loss of ActB resulted in a transient reduction in Olig2$^+$ cell viability in *Inhbb*$^{-/-}$ embryos, and were also compatible with a delay in maturation. Although subtle effects persisted postnatally, this phenotype largely resolved, such that myelination was not delayed.

Delayed myelination in spinal cords of *Smad3*$^{-/-}$ mice

Importantly, examination of *Smad3*$^{-/-}$ mice revealed a more severe oligodendrocyte phenotype, which included delayed myelination (Fig. 8). At E12.5, Olig2$^+$ cells and Sox2$^+$ cells were both reduced in *Smad3*$^{-/-}$ spinal cords (Fig. 8A,B). Olig2$^+$ cells remained diminished at E15.5, encompassing both the parenchymal Olig2$^+$ Sox2$^-$ Sox9$^+$ and periventricular Olig2$^+$ Sox2$^+$ populations (Fig. 8C,D). This reduction persisted at P5 in *Smad3*$^{-/-}$ spinal cords (Fig. 8E-G), and included both Olig2$^+$ Pdgfrα$^+$ OLPs and more mature CC-1$^+$ oligodendrocytes (Fig. 8E). Mag$^+$ cells were also decreased, and expression of Mbp and other mature myelin markers was impaired (Fig. 8E-G). These changes were associated with decreased viability and proliferation. Cleaved caspase-3$^+$ Olig2$^+$ apoptotic cells were substantially increased in *Smad3*$^{-/-}$ spinal cords, and cycling Ki67$^+$ Olig2$^+$ cells were slightly, but significantly, reduced at E12.5 and P5 (Fig. 8H,I). No compensatory

Development (2014) 141, 2414-2428 doi:10.1242/dev.106492

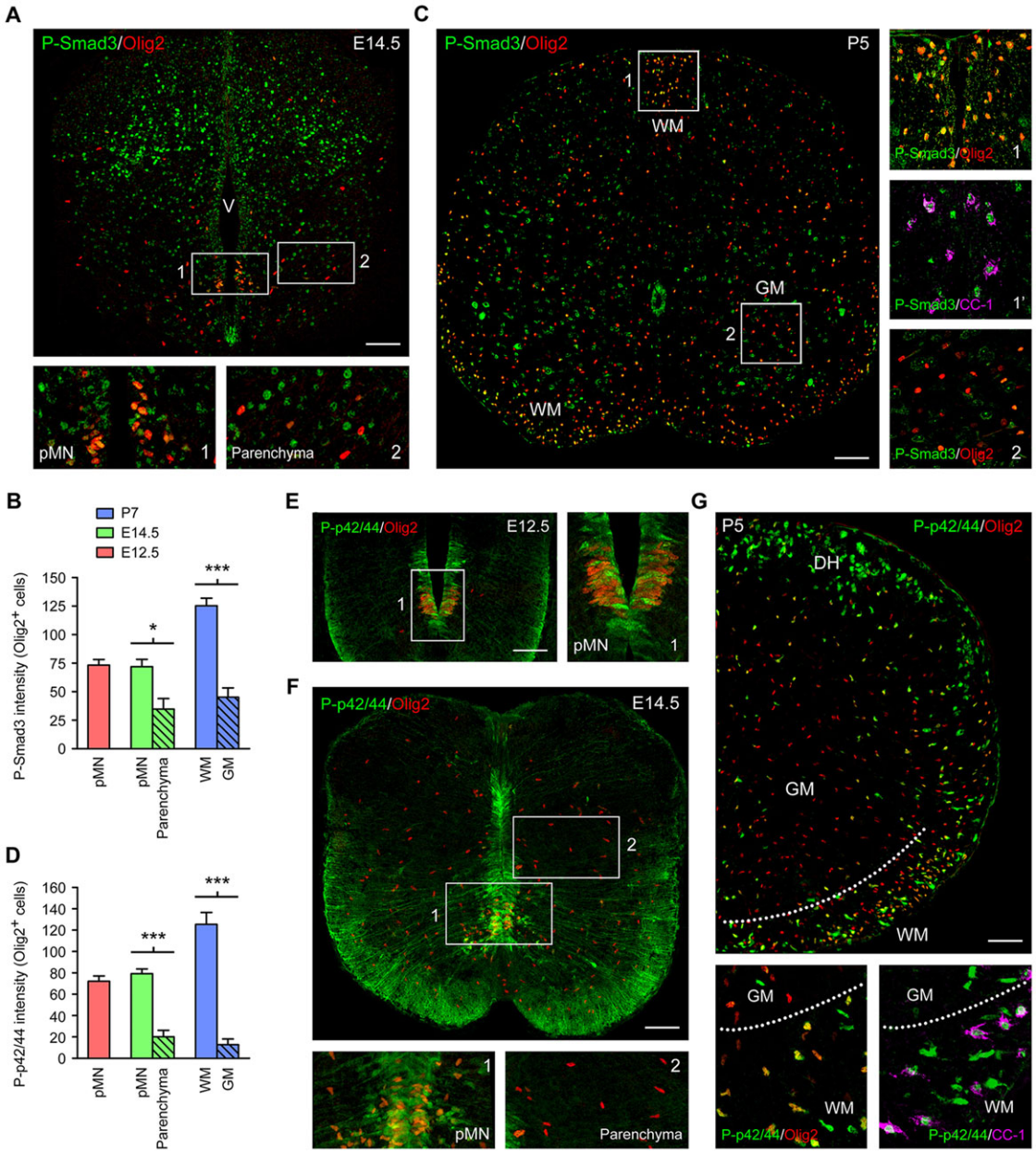

Fig. 5. Maturing oligodendrocytes display strong Smad3 and MAP kinase activity *in vivo*. Analyses of C57BL/6 spinal cords at E12.5, E14.5 and P5, labeled for oligodendrocyte lineage (Olig2) or maturation (CC-1) marker plus Smad3 (P-Ser423/425; A-C) or p42/44 (P-Thr202/Tyr204; D-G). Representative (boxed) areas are labeled and shown at higher magnification. Smad3 activity at E12.5 is illustrated in Fig. 1A. (B,D) Mean pixel intensity for Smad3 (P-Ser423/425; B) or p42/44 (P-Thr202/Tyr204; D) activity measured in Olig2$^+$ cells at each time point. (A,B) Smad3 activity in Olig2$^+$ OLPs in the pMN domain at E14.5 was similar to that at E12.5. Activity was lower in Olig2$^+$ cells migrating into the parenchyma. V, ventricle. (B,C) At P5, at the onset of myelination, strong Smad3 activity was observed in Olig2$^+$ cells in maturing white matter (WM). Activity was lower in Olig2$^+$ cells in gray matter (GM). (C) Representative areas of white matter (dorsal funiculus) and gray matter (ventral horn) are shown at higher magnification. The matching white matter area from an adjacent section is also illustrated, showing that cells positive for maturation markers (CC-1) also displayed strong Smad3 (P-Ser423/425) activity. (D-G) Compatible results were observed for p42/44. At E12.5, p42/44 (P-Thr202/Tyr204) activity localized to cells in the ventral periventricular neuroepithelium including Olig2$^+$ OLPs (D,E), and to radially oriented processes extending to the pial surface (E). A similar pattern was seen at E14.5, and p42/44 activity in Olig2$^+$ cells was similar in the pMN domain at E12.5 and E14.5, but lower in Olig2$^+$ cells in the parenchyma (D,F). (G) At P5, p42/44 (P-Thr202/Tyr204) localized to white matter tracts and neurons within dorsal horns (DH). Activity was high in Olig2$^+$ cells in P5 white matter, but low in gray matter (D,G). (G) The boundary between ventral horn and the ventrolateral funiculus is marked by a dotted line, and a representative area is shown at higher magnification beneath; the matching area from a serial section is also shown, illustrating high p42/44 (P-Thr202/Tyr204) activity in CC-1$^+$ cells. Data are representative of samples from four individuals at each time point. (B,D) Two-way ANOVA plus Bonferroni post-test; *P<0.05, ***P<0.001. Error bars indicate s.e.m. Scale bars: 75 µm in A,E,F; 125 µm in C; 150 µm in G.

induction of Smad2 was observed. No abnormalities were detected in *Smad3*$^{+/-}$ heterozygotes (not shown).

Interestingly, this phenotype also eventually self-corrected, although compensation was delayed. By P28, no differences were detected in Olig2$^+$ or Mag$^+$ cell numbers or in Mbp immunoreactivity in spinal cords of *Smad3*$^{-/-}$ mice versus controls (Fig. 8J,K).

Together, these results demonstrated that loss of Smad3 signaling *in vivo* resulted in a prolonged (but not permanent) reduction in

Development (2014) 141, 2414-2428 doi:10.1242/dev.106492

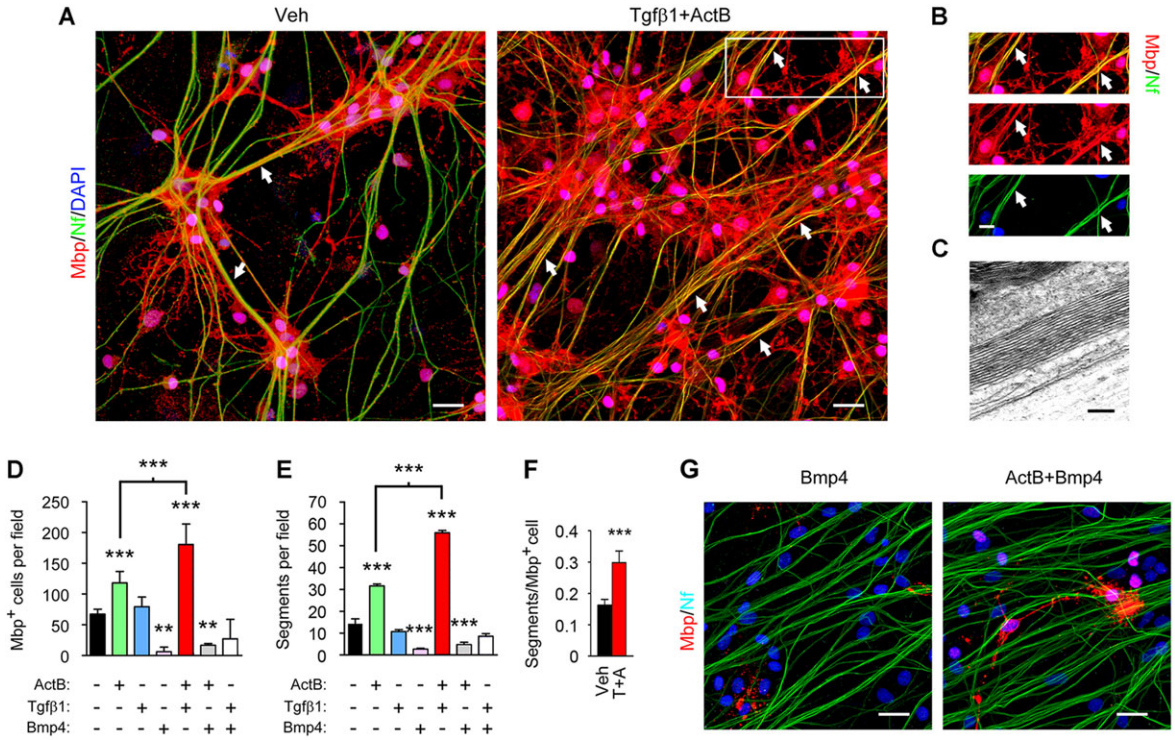

Fig. 6. Tgfβ1 plus ActB co-treatment enhances myelination in OLP-neuron co-cultures. Primary rat OLPs were plated onto DRG neurons and myelination initiated using 1 µg/ml TrkA-Fc, then co-cultures treated with 50 ng/ml ActB, Tgfβ1 and/or Bmp4 over 14 days and analyzed by confocal imaging and morphometry (A,B), supported by electron microscopy (C). At 14 days, control and ActB-treated and/or Tgfβ1-treated co-cultures contained mature Mbp^+ oligodendrocytes, the processes of which co-localized with neurofilament$^+$ (Nf^+) axons to form linear Mbp^+ Nf^+ profiles corresponding to compact myelin segments (A,B), as confirmed by electron microscopy (C). Examples of Mbp^+ Nf^+ profiles are arrowed in A, and the boxed area in the right panel (from co-treated co-cultures) is shown at higher magnification in B. ActB-treated co-cultures contained more Mbp^+ cells and myelin segments than controls, whereas Tgfβ1 had no effect (D,E). However, co-treatment with Tgfβ1 plus ActB resulted in a marked increase in Mbp^+ cells and segments beyond ActB alone (A,D,E). Numbers of myelin segments per Mbp^+ cell were also increased in ActB-treated or co-treated cultures (F; T+A, Tgfβ1 plus ActB co-treatment). Conversely, co-cultures exposed to Bmp4 contained almost no Mbp^+ cells or myelin segments, even in the presence of ActB co-treatment (D,E,G). Data are representative of three independent experiments in separate co-cultures. (D,E) One-way ANOVA plus Bonferroni post-test; $^{**}P<0.01$, $^{***}P<0.001$, versus control unless otherwise indicated. Error bars indicate s.e.m. Scale bars: 10 µm in A,G; 5 µm in B; 150 nm in C.

oligodendrocyte lineage cells that was associated with persistently impaired viability and proliferation, decreased numbers of progenitors and mature cells, and delayed myelination.

Tgfβ1 and ActB promote neural progenitor viability *in vitro*

Since the phenotype of *Smad3*$^{-/-}$ mice included effects on $Sox2^+$ progenitors, we examined outcomes of Tgfβ1 treatment in primary neural progenitor cultures (supplementary material Fig. S6). ActB was included for comparison, although it does not overlap the periventricular zone in early embryogenesis. Adherent cultures were grown in media favoring proliferation (containing Egf) or specification and differentiation (growth factor-free), in the presence of 1-100 ng/ml Tgfβ1, ActB or vehicle (Conti et al., 2005; Louis et al., 2013). Cells positive for the neural progenitor marker nestin, Olig2, caspase cleavage and BrdU-labeling were quantified at 12 h and 60 h in proliferation media and at 96 h in differentiation media.

Notably, both Tgfβ1 and ActB improved neural progenitor viability in these studies, in the absence and in the presence of Egf. ActB and Tgfβ1 both reduced the numbers and fraction of cleaved caspase-3^+ cells under both culture conditions (supplementary material Fig. S6A,B). However, Egf has been reported as crucial for neural progenitor proliferation, and neither Tgfβ1 nor ActB impacted the $BrdU^+$ fraction in Egf-containing media (supplementary material Fig. S6C) nor was able to rescue proliferation in Egf-free media (supplementary material Fig. S6D). In addition, neither ligand affected oligodendrocyte lineage specification. No $Olig2^+$ cells were observed in proliferation medium under any condition, with the population remaining entirely nestin$^+$ (supplementary material Fig. S6E). Under conditions favoring lineage specification and differentiation, at 96 h ~30% of cells were $Olig2^+$, and this was unchanged by ActB or Tgfβ1 treatment (supplementary material Fig. S6F).

Together, these results suggested that Tgfβ1 and ActB promote neural progenitor viability, compatible with outcomes in specified OLPs, but we detected no impact on proliferation or oligodendrocyte lineage specification.

DISCUSSION

Smad3 signaling supports myelination in the developing spinal cord

In this study, we show that combinatorial signaling by Tgfβ and Activin ligands supports oligodendrocyte development and CNS myelination. Using mouse spinal cord as a model system, we found that at E12.5, following ventral OLP specification, canonical Smad3 activity localizes to the $Sox2^+$ periventricular zone, including $Olig2^+$ OLPs in the pMN domain. Our data suggest that Smad3 activity in the oligodendrocyte lineage is likely to result initially from exposure to Tgfβ1-3 in the periventricular neuroepithelium, then later from combined exposure to Tgfβ plus ActB in the parenchyma, particularly during differentiation in late embryogenesis and the early postnatal

Development (2014) 141, 2414-2428 doi:10.1242/dev.106492

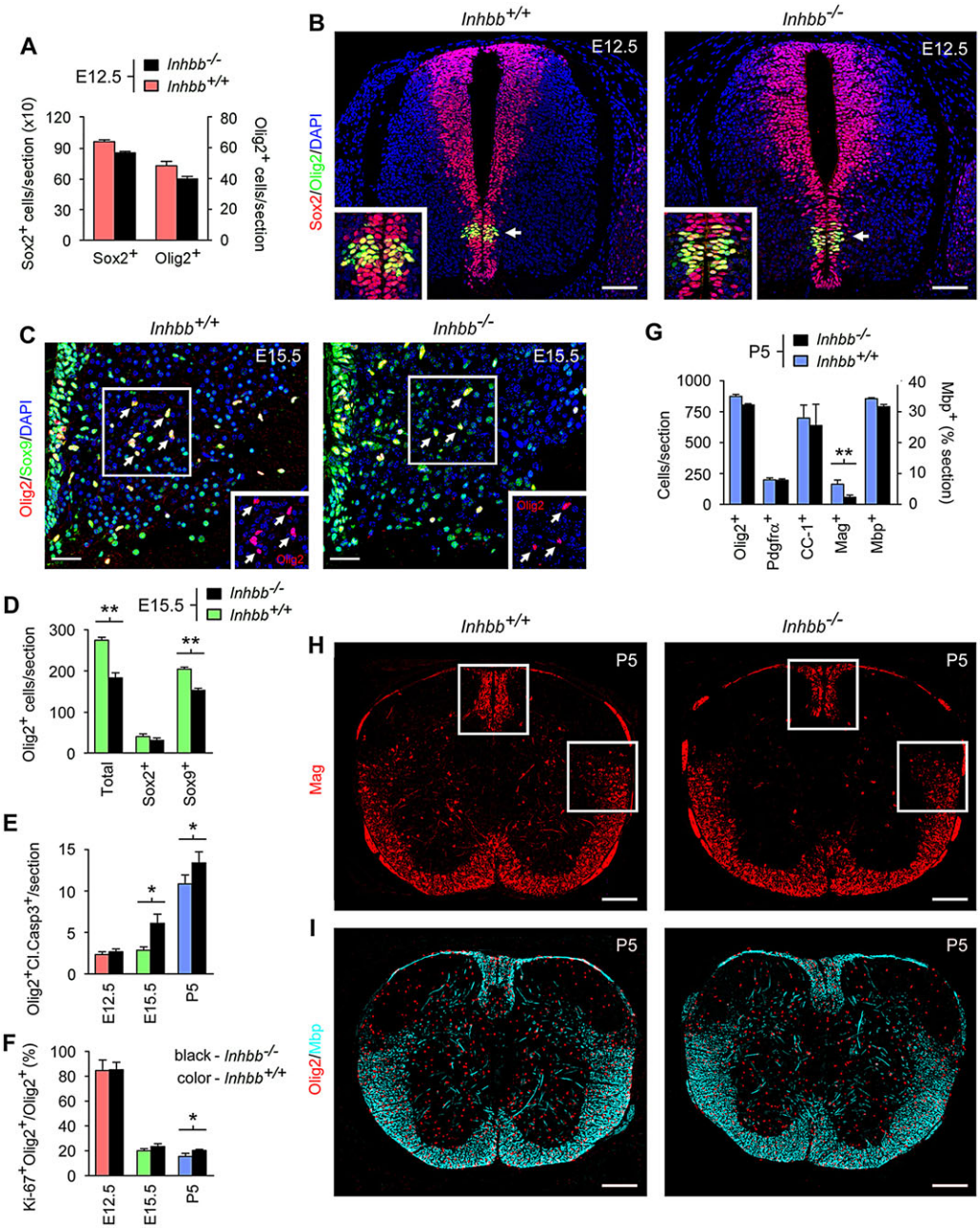

Fig. 7. Transient impairment of oligodendrocyte development in *Inhbb*$^{-/-}$ spinal cord. Analyses of immunolabeled spinal cord sections from *Inhbb*$^{-/-}$ mice and littermate controls, from E12.5 through P5. At E12.5, numbers of Olig2$^+$ OLPs were not significantly decreased in *Inhbb*$^{-/-}$ samples (A,B), but by E15.5 were lower than in controls (C,D). (B) pMN domains are arrowed and magnified in the inset. (C) Representative areas of parenchyma are outlined, and Olig2$^+$ cells (red channel, arrows) are shown in the inset. At E15.5, numbers of Olig2$^+$ Sox2$^-$ Sox9$^+$ OLPs within the parenchyma were reduced (C,D), whereas no change was seen in early Olig2$^+$ Sox2$^+$ OLPs remaining in periventricular neuroepithelium (D). At E15.5, cleaved caspase-3$^+$ Olig2$^+$ apoptotic cells were increased in *Inhbb*$^{-/-}$ samples (E), whereas the fraction of proliferating Ki67$^+$ Olig2$^+$ cells was unaltered (F). At P5, apoptotic Olig2$^+$ cells remained elevated, and the fraction of Ki67$^+$ Olig2$^+$ cells was marginally but significantly raised (E,F). However, numbers of Olig2$^+$ cells in *Inhbb*$^{-/-}$ and control cords were similar (G-I), and no differences were detected in Olig2$^+$ Pdgfrα$^+$ OLPs or mature CC-1$^+$ Olig2$^+$ oligodendrocytes (G). Cells expressing the early myelin protein Mag were reduced, but Mbp immunoreactivity was normal (G-I). (H) Dorsal and lateral funiculi of P5 spinal cords labeled for Mag are outlined to highlight differences. Data are representative of samples from four individuals per genotype per time point. Student's *t*-test (A,D,G) or two-way ANOVA plus Bonferroni post-test (E,F); **P*<0.05, ***P*<0.01. Error bars indicate s.e.m. Scale bars: 50 µm in B; 15 µm in C; 250 µm in H,I.

period. We show that Tgfβ1 and ActB differentially activate canonical Smad3 and non-canonical Smad-independent MAP kinase signaling in OLPs *in vitro*, and that co-treatment produces a third response, strongly activating both signaling pathways. Moreover, each pattern correlates with a distinct functional outcome. Each ligand inhibits apoptosis, and Tgfβ promotes proliferation whereas ActB enhances maturation. In combination, they further enhance viability, and their effects on proliferation and maturation are combined, resulting in a potent increase in mature oligodendrocytes. Co-treatment promotes myelination in OLP-neuron co-cultures, and maturing oligodendrocytes in myelinating spinal cord are strongly positive for Smad3 and MAP kinase activation. In mice, inactivation of ActB

Development (2014) 141, 2414-2428 doi:10.1242/dev.106492

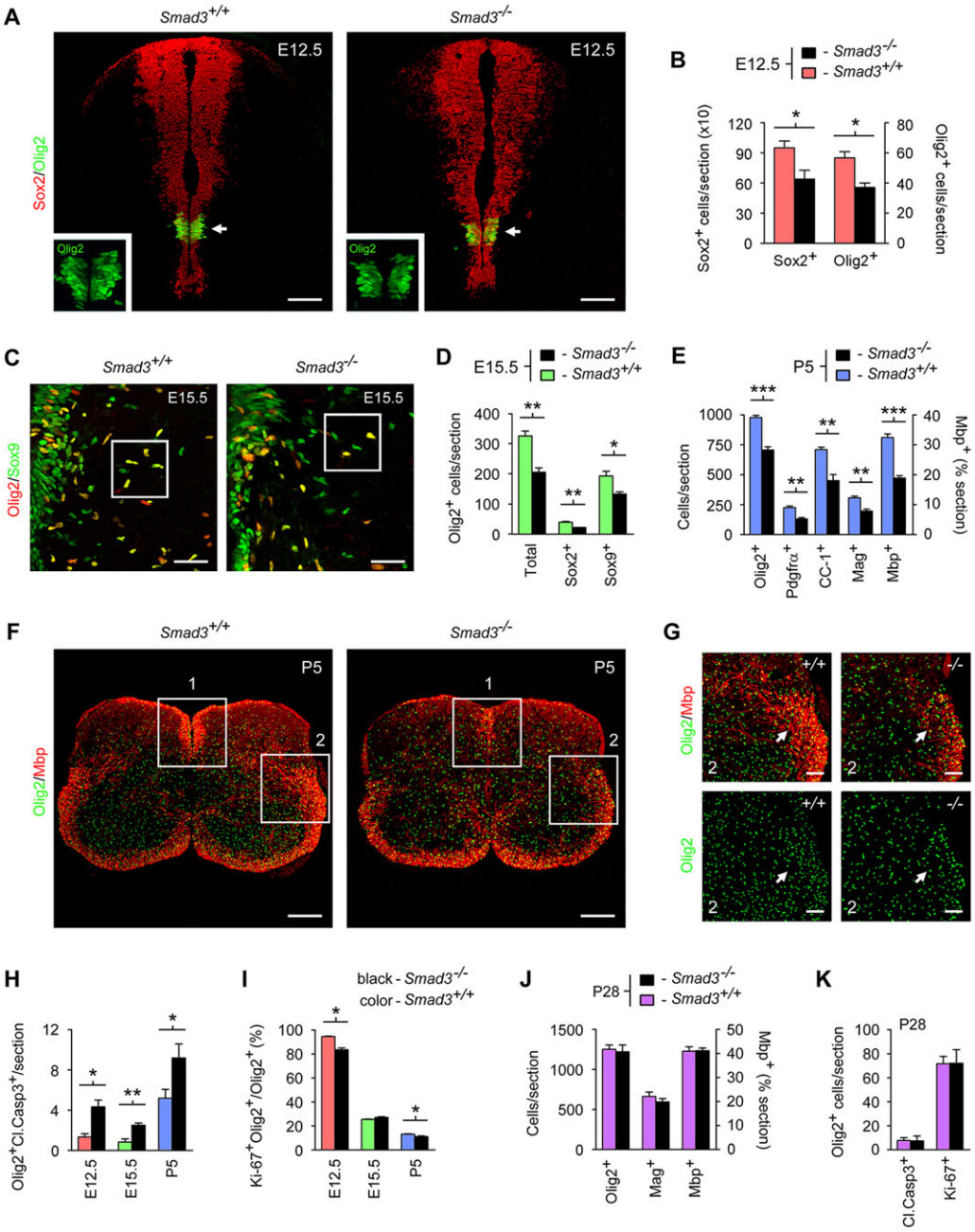

Fig. 8. Delayed myelination in spinal cords of *Smad3*$^{-/-}$ mice. Analyses of immunolabeled spinal cord sections from *Smad3*$^{-/-}$ mice and littermate controls from E12.5 through P28. (A,B) At E12.5, Olig2$^+$ OLPs and Sox2$^+$ cells were significantly reduced in *Smad3*$^{-/-}$ samples. (C,D) Olig2$^+$ cells were also reduced at E15.5, including both the parenchymal Olig2$^+$ Sox2$^-$ Sox9$^+$ and early periventricular Olig2$^+$ Sox2$^+$ populations. (A) pMN domains are arrowed, and Olig2$^+$ cells (green channel) are shown in the inset. (C) Representative areas of parenchyma are outlined. (E-G) The decrease in Olig2$^+$ cells in *Smad3*$^{-/-}$ spinal cord persisted at P5 and encompassed Olig2$^+$ Pdgfrα$^+$ OLPs and mature Olig2$^+$ CC-1$^+$ cells (E). Mag$^+$ cells were decreased (E) and Mbp significantly reduced (E-G). (F) Dorsal and lateral funiculi of P5 spinal cords labeled for Mbp and Olig2 are outlined to highlight differences, and lateral funiculi are shown at higher magnification in G, with representative areas arrowed. (H,I) Analyses of apoptotic and proliferating Olig2$^+$ cells from E12.5 through P5. Apoptotic Olig2$^+$ cells were substantially and persistently increased in *Smad3*$^{-/-}$ samples (H), while the fraction of Ki67$^+$ Olig2$^+$ cells was slightly reduced at E12.5 and postnatally (I). (J,K) The white matter phenotype of *Smad3*$^{-/-}$ spinal cords self-corrected by P28, at which time no significant abnormalities were detected in Olig2$^+$ or Mag$^+$ cell number or Mbp immunoreactivity. Data are representative of four individuals per genotype per time point. Student's *t*-test (B,D,E,J,K) or two-way ANOVA plus Bonferroni post-test (H,I); **P*<0.05, ***P*<0.01, ****P*<0.001. Error bars indicate s.e.m. Scale bars: 50 µm in A; 20 µm in C; 250 µm in F; 25 µm in G.

alone results in a transient reduction in Olig2$^+$ cells and increased apoptosis, but numbers, differentiation and myelination rapidly recover. Importantly, in *Smad3*$^{-/-}$ mice, the numbers of mature and immature Olig2$^+$ cells are more persistently reduced, indices of viability and proliferation are diminished, and myelination is delayed.

Smad3 activity in Olig2$^+$ OLPs in periventricular neuroepithelium of mouse spinal cord

Our expression data are compatible with and extend previous studies. ActrIIb has been reported in mouse and chick neural tube at time points including those of OLP specification (Feijen et al., 1994; Stern et al., 1995), and the data from mouse match our own findings. *Inhbb*

Development (2014) 141, 2414-2428 doi:10.1242/dev.106492

mRNA has been detected in mouse neural tube at similar time points (Feijen et al., 1994), although the longitudinal sections presented render comparison with our own results difficult. Interestingly, *in situ* hybridization studies in chick have also reported *Smad3* mRNA within periventricular neuroepithelium, although the signal in the pMN domain was relatively low at HH stages 25-26 (E4.5-5.0, equivalent to mouse E13), and absent at stages 12-18 (E2.0-3.0, equivalent to mouse E10-11.5) (Garcia-Campmany and Marti, 2007; Estaras et al., 2012). In the chick, OLPs emerge from ventral neuroepithelium as in rodents, beginning at E6.0 (HH stages 28-29) (Ono et al., 1995). In our studies in mouse, the double-labeling data confirm Smad3 expression and activity (P-Ser423/425) at E12.5 in OLPs in the pMN domain, compatible with the pattern throughout the periventricular neuroepithelium, and these findings also match our data for Tgfβr2 and Tgfβ1-3, which are compatible with previous reports (Flanders et al., 1991; Mecha et al., 2008). Thus, in mouse, the ligands, receptor and active form of the transcription factor are present at E12.5 throughout the periventricular neuroepithelium, including $Olig2^+$ cells in the pMN domain. Whether a slight species difference exists in the timing of Smad3 expression and oligodendrocyte generation is not yet clear, and comparative studies will be needed to resolve this question.

Transition of Tgfβ and Activin signaling *in vivo* – from distinct to overlapping patterns

We tracked longitudinal changes in expression within spinal cord and, importantly, these analyses revealed that during embryogenesis the patterns of Tgfβ1 versus ActB switch from differential to overlapping, and are reflected in changes in Smad3 and MAP kinase activity, although an important qualifier is that MAP kinase pathways are also activated by factors beyond the Tgfβ superfamily (Bhat and Zhang, 1996; Althaus et al., 1997; Yim et al., 2001). Our mechanistic experiments demonstrate functional responses to these ligands individually and in combination, and our data from $Inhbb^{-/-}$ and $Smad3^{-/-}$ mice are compatible with these outcomes. That the $Smad3^{-/-}$ phenotype is the more severe might be attributable to complete versus partial ablation of Tgfβ/Activin Smad-dependent signaling. The compensation seen in both genotypes also follows a precedent in other models displaying deficits in oligodendrocyte development and/or myelination (Montag et al., 1994; Larsen et al., 2006; Lewallen et al., 2011), although recovery is not a universal outcome (Meyerheim et al., 2004; Nolan et al., 2005; Emery et al., 2009). Our findings are also compatible with data from previous studies in mutants for MAP kinase components (Schwammenthal et al., 2004; Fyffe-Maricich et al., 2011).

Notably, our data do not exclude potential contributions from other ligand-receptor combinations known to induce Smad3 activation, and such contributions would not discount the significance of our findings. Our data demonstrate that combinatorial effects of Smad3-activating ligands enhance oligodendrocyte development. Moreover, and importantly, we show that the net impact of Smad3 signaling *in vivo* (from all potential sources) promotes myelination in mammalian spinal cord.

Roles of Tgfβ and Activin ligands in oligodendrocyte development

The impact of ActB and Tgfβ1 on OLP viability and differentiation in our *in vitro* experiments is compatible with the findings of previous studies in CNS neuronal cultures (Schubert et al., 1990; Poulsen et al., 1994; Krieglstein et al., 1995; Cambray et al., 2012). Reports also suggest potential roles for Tgfβ and Activin ligands in repair in demyelinating models (Hinks and Franklin, 1999; John et al., 2002; Miron et al., 2013). Interestingly, however, our data do not match a report in Oli-Neu cells that implicated ActA in the causation of apoptosis (Schulz et al., 2008). Although ActA is not found in the developing CNS (Feijen et al., 1994), in our own experiments in primary OLPs we have found that it produces a close match to the effects of ActB, and so the source of this dichotomy is not immediately clear. Our findings showing that Tgfβ1 supports OLP proliferation are compatible with results in Schwann cells, in which it also acts as a mitogen (Ridley et al., 1989; Einheber et al., 1995). However, in studies in aggregate CNS cultures, addition of Tgfβ1 has been shown to enhance myelination (Diemel et al., 2003), whereas Tgfβ1 inhibition potentiates platelet-derived growth factor-aa (Pdgf-aa)-driven proliferation in O-2A cells (McKinnon et al., 1993). Notably, aggregate cultures are known to contain Tgfβ-producing cells, and, based on our data, ActB would also likely be present. Based on our results, addition of Tgfβ1 in the presence of ActB might be expected to lead to an overall increase in mature oligodendrocytes; thus, the two studies might be compatible. While the extent to which O-2A cells are representative of specified OLPs is not clear, we carefully examined effects on proliferation in our experiments in $Smad3^{-/-}$ mice. Since Pdgfrα signaling is an important mitogen for OLPs (Raff et al., 1988), we examined whether *Smad3* inactivation *in vivo* would result in detectable changes in OLP proliferation and, if so, whether a decrease or increase would result. However, we detected significant reductions in the fraction of $Ki67^+$ $Olig2^+$ cells in $Smad3^{-/-}$ samples at both E12.5 and postnatally, compatible with our results in OLP cultures.

Tgfβ and Activin signaling in white matter formation

Taken together, our findings suggest a model of how Smad3-activating ligands might contribute to oligodendrocyte development in mammalian spinal cord. Initially, Tgfβ ligand-activated canonical and non-canonical signaling might support viability and proliferation in specified OLPs. As these cells spread dorsally within the cord, they remain under the influence of Tgfβ ligands, and also encounter ActB within the parenchyma. The combination of Tgfβ and Activin signaling further promotes viability, and effects on proliferation and maturation are combined, resulting in increased numbers of mature cells available for myelination.

MATERIALS AND METHODS

Antibodies

Phospho-Smad2 (Ser465/467), Smad2, phospho-Smad1/5/8 (Ser463/465), Smad3, phospho-Smad3, cleaved caspase-3, phospho-Gsk3α/β (Ser21/9), p38 (Mapk14), phospho-p38 (Thr180/Tyr182), phospho-p44/42 (Mapk3/1) (Thr202/Tyr204) and Foxh1 (FAST) were from Cell Signaling. Tgfβr2, Tgfβ1, Tgfβ2, Tgfβ3, Pdgfrα, β-actin, Bmpr2, rabbit IgG and mouse IgG were from Santa Cruz Biotechnology. Cnpase, Olig2, Ki67, Lim1 (Lhx1), Sox9, nestin, Sox2, NeuN (Rbfox3) were from Millipore. Other antibodies: Mbp was from Dako; Mbp, mouse CC-1 (Apc) and Gfap were from Abcam; Mag was from Dr Jim Salzer (NYU); BrdU was from Immunology Consultants; ActrIIa (Acvr2a) and ActrIIb (Acvr2b) were from Abbiotec; Isl2 and Mnr2 (Mnx1) were from DSHB (University of Iowa); Inhba and Inhbb were from Proteintech. Please see supplementary material Table S1 for a complete list of antibodies used, species, dilutions and catalog numbers.

Cytokines/growth factors

Human ACTB, TGFβ1 and BMP4 were from Peprotech and used at 1-100 ng/ml. EGF was from Invitrogen and used at 20 ng/ml.

OLP cultures

OLPs were purified from cortices of P2 Sprague Dawley rats as reported (Caporaso and Chao, 2001). At plating, these cultures are >95% $Olig2^+$ $A2B5^+$ $Pdgfrα^+$ $Cnpase^-$ Mbp^- OLPs (Gurfein et al., 2009). Cells were

Development (2014) 141, 2414-2428 doi:10.1242/dev.106492

plated in minimal essential medium (MEM) plus 15% FBS (Gibco), then changed to serum-free Bottenstein-Sato medium (Gibco) and continuously exposed to 1-100 ng/ml Tgfβ1, ActB and/or Bmp4 for up to 5 days.

Myelinating co-cultures

DRG neurons were isolated from E16.5 rat embryos as reported (Chan et al., 2004). Rat OLPs (as above) were then plated onto DRG neurons and myelination induced using 1 μg/ml TrkA-Fc (Chan et al., 2004). Co-cultures were fixed at 14 days to assess myelination.

Adherent neural progenitor cultures

The protocol and proprietary reagents from STEMCELL Technologies were used to generate monolayer neural progenitor cultures (Conti et al., 2005; Louis et al., 2013). Ganglionic eminences from E14 mouse embryos were dissected and triturated, and dissociated cells plated into proprietary proliferation media containing 20 ng/ml recombinant human EGF (Invitrogen). To induce differentiation, cells were plated into proprietary growth factor-free media for up to 96 h.

Bromodeoxyuridine (BrdU) incorporation

10 μM BrdU (BD Biosciences) was added to cells 12 h prior to fixation. Cells were stained for BrdU as per the manufacturer's instructions.

Immunoblotting and co-immunoprecipitation

SDS-PAGE and immunoblotting were carried out as described (Zhang et al., 2011). Co-immunoprecipitation for Smad3 or using IgG control was performed in Oli-Neu or HEK cell cultures using previously reported protocols (Attisano et al., 2001).

Immunocytochemistry

OLP or neural progenitor cultures, and OLP-neuron co-cultures, were fixed for 10 min with 4% paraformaldehyde and immunostained as previously described (Zhang et al., 2006, 2009). For surface antigens, PBS was used as buffer. For intracellular antigens, PBS containing 0.3% Triton X-100 was used.

Mice

Inhbb$^{-/-}$ mice were made by Dr Rudolf Jaenisch (MIT) and display failure of eyelid fusion and impaired female reproduction (Vassalli et al., 1994). *Smad3*$^{ex8/ex8}$ (*Smad3*$^{-/-}$) mice were made by Dr Chuxia Deng (NIH) and are immunodeficient and die before 8 months of age (Yang et al., 1999). C57BL/6 mice were from Taconic. Experiments involving animals were approved by the Institutional Animal Care and Use Committee, and conformed to institutional and national animal welfare laws, guidelines and policies.

Immunohistochemistry

Frozen sections were rehydrated in PBS, then subjected to epitope retrieval in citrate buffer (pH 6) at 95-100°C for 10-15 min and immunostained using published protocols (Zhang et al., 2006, 2009).

Morphometric analysis

Differentiation, proliferation and apoptosis in OLP or neural progenitor cultures was quantified in *z*-series stacks at 20×. Positive cells were counted in five 20× fields of vision per condition by a blinded observer and data compared statistically. In OLP-neuron co-cultures, myelin segments were identified as Mbp$^+$ linear profiles extending along Nf$^+$ axons. Number and length were quantified by a blinded observer in five stacks per condition. To characterize expression patterns in wild-type mouse embryos and the phenotypes of *Inhbb*$^{-/-}$ and *Smad3*$^{ex8/ex8}$ mice, cell number, myelinated area, or mean pixel intensity in cells marked with lineage or maturation markers were carried out in at least three fields in images of immunolabeled sections at 20× magnification per animal, three animals per genotype or condition per time point, in at least three independent experiments per study by a blinded observer.

Modeling

A previously described model (Zhang et al., 2011; Hsieh et al., 2004) was adapted to separate effects of ActB on OPC proliferation, apoptosis and differentiation (Fig. 4). The model calculates the proliferation coefficients of the Olig2$^+$ Mbp$^-$ (OLP plus immature) (α) and mature Olig2$^+$ Mbp$^+$ oligodendrocyte populations (γ), differentiation from one to the other (β), and the net coefficient of apoptosis of OLPs plus mature cells δ+ε) (Fig. 4A). These take into account the rate of change of the measured parameters and the size of the population (Hsieh et al., 2004).

The model uses differential equations to generate coefficients α through ε:

$$\mathbf{d}N^{OLP}/\mathbf{d}t = (\boldsymbol{\alpha} - \boldsymbol{\delta})N^{OLP} - \boldsymbol{\beta}N^{OLP}, \quad (1)$$

the change in OLP percentage (N^{OLP}) over time.

$$\mathbf{d}N^{MBP}/\mathbf{d}t = (\boldsymbol{\gamma} - \boldsymbol{\varepsilon})N^{MBP} + \boldsymbol{\beta}N^{OLP}, \quad (2)$$

the change in mature cell percentage (N^{MBP}) over time.

$$\mathbf{d}N^{Total}/\mathbf{d}t = (\boldsymbol{\alpha} - \boldsymbol{\delta})N^{OLP} + (\boldsymbol{\gamma} - \boldsymbol{\varepsilon})N^{MBP}, \quad (3)$$

the change in total cell number over time.

$$BrdU_{i+1} = 2\gamma_i N_i^{MBP} + 2\alpha_i N_i^{OLP}, \quad (4)$$

mitotic cells (BrdU$^+$) between times i and i+1.

$$BrdU_{i+1}^{OLP} = 2\alpha_i N_i^{OLP} - \beta_i[\alpha_i/(1+\alpha_i)]N_i^{OLP} \quad \text{and} \quad (5)$$

$$BrdU_{i+1}^{MBP} = 2\gamma_i N_i^{MBP} + \beta_i[\alpha_i/(1+\alpha_i)]N_i^{OLP}, \quad (6)$$

the percentage of mitotic OLPs and mature Mbp$^+$ cells between times i and i+1.

The model was validated by comparison of predicted versus measured values for total cells and differentiation (Eq. 3) at 12 h intervals from 12 h and 120 h in untreated cultures.

Statistical analyses

Data represent mean±s.e.m. For multiple comparisons, ANOVA plus Bonferroni post test was used. Two-tailed Student's *t*-test was used to compare two groups of matched samples. $P<0.05$ was considered significant.

Acknowledgements

We thank the laboratory of Dr Fred H. Gage (Salk Institute, USA) for assistance with designing the mathematical model included in this work. We thank Rumana Haq, Lauren O'Rourke and Dr Victor Friedrich of the MSSM Microscopy Facility for assistance with imaging.

Competing interests

The authors declare no competing financial interests.

Author contributions

D.J.D. performed experiments, analyzed data and wrote the manuscript. A.Z., J.N.M., J.Z., L.A., J.H., S.M., B.M.L., A.T.A. and M.U. performed experiments and analyzed data. N.M. analyzed data. F.H. designed and performed mathematical modeling analyses. C.V.M.-V., P.C., E.P.B. and C.W.B. designed experiments and edited the manuscript. G.R.J. designed experiments and wrote the manuscript.

Funding

This work was supported by the National Institutes of Health [R01NS056074 and R01NS062703 to G.R.J., U01DK060995, R01DK056077, R01DK073960, R01DK060043 and DK060043-S1 to E.P.B., R01HD01156 and R01HD27823 to C.W.B., R01NS52738 and R37NS42925 to P.C., SC1NS000001 to C.V.M.-V. and R24CA095823 to the MSSM Microscopy Facility]. Additional support was provided by National MS Society [RG3874 and RG4127 to G.R.J. and FG2005 to L.A.]; the Beker Foundation (G.R.J.); Noto Foundation (G.R.J.); Robert Wood Johnson Foundation (C.W.B.); and March of Dimes [5-FY01-482 to C.W.B.]. Deposited in PMC for release after 12 months.

Supplementary material

Supplementary material available online at
http://dev.biologists.org/lookup/suppl/doi:10.1242/dev.106492/-/DC1

References

Althaus, H. H., Hempel, R., Klöppner, S., Engel, J., Schmidt-Schultz, T., Kruska, L. and Heumann, R. (1997). Nerve growth factor signal transduction in mature pig oligodendrocytes. *J. Neurosci. Res.* **50**, 729-742.

Attisano, L., Silvestri, C., Izzi, L. and Labbé, E. (2001). The transcriptional role of Smads and FAST (FoxH1) in TGFbeta and activin signalling. *Mol. Cell. Endocrinol.* **180**, 3-11.

Bhat, N. R. and Zhang, P. (1996). Activation of mitogen-activated protein kinases in oligodendrocytes. *J. Neurochem.* **66**, 1986-1994.
Cai, J., Qi, Y., Hu, X., Tan, M., Liu, Z., Zhang, J., Li, Q., Sander, M. and Qiu, M. (2005). Generation of oligodendrocyte precursor cells from mouse dorsal spinal cord independent of Nkx6 regulation and Shh signaling. *Neuron* **45**, 41-53.
Cambray, S., Arber, C., Little, G., Dougalis, A. G., de Paola, V., Ungless, M. A., Li, M. and Rodríguez, T. A. (2012). Activin induces cortical interneuron identity and differentiation in embryonic stem cell-derived telencephalic neural precursors. *Nat. Commun.* **3**, 841.
Caporaso, G. L. and Chao, M. V. (2001). Telomerase and oligodendrocyte differentiation. *J. Neurobiol.* **49**, 224-234.
Chan, J. R., Watkins, T. A., Cosgaya, J. M., Zhang, C., Chen, L., Reichardt, L. F., Shooter, E. M. and Barres, B. A. (2004). NGF controls axonal receptivity to myelination by Schwann cells or oligodendrocytes. *Neuron* **43**, 183-191.
Chen, X., Rubock, M. J. and Whitman, M. (1996). A transcriptional partner for MAD proteins in TGF-beta signalling. *Nature* **383**, 691-696.
Conti, L., Pollard, S. M., Gorba, T., Reitano, E., Toselli, M., Biella, G., Sun, Y., Sanzone, S., Ying, Q.-L., Cattaneo, E. et al. (2005). Niche-independent symmetrical self-renewal of a mammalian tissue stem cell. *PLoS Biol.* **3**, e283.
De Robertis, E. M. and Kuroda, H. (2004). Dorsal-ventral patterning and neural induction in Xenopus embryos. *Annu. Rev. Cell Dev. Biol.* **20**, 285-308.
Diemel, L. T., Jackson, S. J. and Cuzner, M. L. (2003). Role for TGF-beta1, FGF-2 and PDGF-AA in a myelination of CNS aggregate cultures enriched with macrophages. *J. Neurosci. Res.* **74**, 858-867.
Einheber, S., Hannocks, M. J., Metz, C. N., Rifkin, D. B. and Salzer, J. L. (1995). Transforming growth factor-beta 1 regulates axon/Schwann cell interactions. *J. Cell Biol.* **129**, 443-458.
Emery, B., Agalliu, D., Cahoy, J. D., Watkins, T. A., Dugas, J. C., Mulinyawe, S. B., Ibrahim, A., Ligon, K. L., Rowitch, D. H. and Barres, B. A. (2009). Myelin gene regulatory factor is a critical transcriptional regulator required for CNS myelination. *Cell* **138**, 172-185.
Estaras, C., Akizu, N., Garcia, A., Beltran, S., de la Cruz, X. and Martinez-Balbas, M. A. (2012). Genome-wide analysis reveals that Smad3 and JMJD3 HDM co-activate the neural developmental program. *Development* **139**, 2681-2691.
Fancy, S. P. J., Chan, J. R., Baranzini, S. E., Franklin, R. J. M. and Rowitch, D. H. (2011). Myelin regeneration: a recapitulation of development? *Annu. Rev. Neurosci.* **34**, 21-43.
Feijen, A., Goumans, M. J. and van den Eijnden-van Raaij, A. J. (1994). Expression of activin subunits, activin receptors and follistatin in postimplantation mouse embryos suggests specific developmental functions for different activins. *Development* **120**, 3621-3637.
Flanders, K. C., Ludecke, G., Engels, S., Cissel, D. S., Roberts, A. B., Kondaiah, P., Lafyatis, R., Sporn, M. B. and Unsicker, K. (1991). Localization and actions of transforming growth factor-beta s in the embryonic nervous system. *Development* **113**, 183-191.
Fogarty, M., Richardson, W. D. and Kessaris, N. (2005). A subset of oligodendrocytes generated from radial glia in the dorsal spinal cord. *Development* **132**, 1951-1959.
Fragoso, G., Haines, J. D., Roberston, J., Pedraza, L., Mushynski, W. E. and Almazan, G. (2007). p38 mitogen-activated protein kinase is required for central nervous system myelination. *Glia* **55**, 1531-1541.
Funaba, M., Zimmerman, C. M. and Mathews, L. S. (2002). Modulation of Smad2-mediated signaling by extracellular signal-regulated kinase. *J. Biol. Chem.* **277**, 41361-41368.
Fyffe-Maricich, S. L., Karlo, J. C., Landreth, G. E. and Miller, R. H. (2011). The ERK2 mitogen-activated protein kinase regulates the timing of oligodendrocyte differentiation. *J. Neurosci.* **31**, 843-850.
Garcia-Campmany, L. and Marti, E. (2007). The TGFbeta intracellular effector Smad3 regulates neuronal differentiation and cell fate specification in the developing spinal cord. *Development* **134**, 65-75.
Grimm, O. H. and Gurdon, J. B. (2002). Nuclear exclusion of Smad2 is a mechanism leading to loss of competence. *Nat. Cell Biol.* **4**, 519-522.
Gurfein, B. T., Zhang, Y., Lopez, C. B., Argaw, A. T., Zameer, A., Moran, T. M. and John, G. R. (2009). IL-11 regulates autoimmune demyelination. *J. Immunol.* **183**, 4229-4240.
Hinks, G. L. and Franklin, R. J. M. (1999). Distinctive patterns of PDGF-A, FGF-2, IGF-I, and TGF-beta1 gene expression during remyelination of experimentally-induced spinal cord demyelination. *Mol. Cell. Neurosci.* **14**, 153-168.
Hsieh, J., Aimone, J. B., Kaspar, B. K., Kuwabara, T., Nakashima, K. and Gage, F. H. (2004). IGF-I instructs multipotent adult neural progenitor cells to become oligodendrocytes. *J. Cell Biol.* **164**, 111-122.
John, G. R., Shankar, S. L., Shafit-Zagardo, B., Massimi, A., Lee, S. C., Raine, C. S. and Brosnan, C. F. (2002). Multiple sclerosis: re-expression of a developmental pathway that restricts oligodendrocyte maturation. *Nat. Med.* **8**, 1115-1121.
Kato, T., Ohtani-Kaneko, R., Ono, K., Okado, N. and Shiga, T. (2005). Developmental regulation of activated ERK expression in the spinal cord and dorsal root ganglion of the chick embryo. *Neurosci. Res.* **52**, 11-19.
Kretzschmar, M., Doody, J., Timokhina, I. and Massague, J. (1999). A mechanism of repression of TGFbeta/Smad signaling by oncogenic Ras. *Genes Dev.* **13**, 804-816.
Krieglstein, K., Suter-Crazzolara, C., Fischer, W. H. and Unsicker, K. (1995). TGF-beta superfamily members promote survival of midbrain dopaminergic neurons and protect them against MPP+ toxicity. *EMBO J.* **14**, 736-742.
Larsen, P. H., DaSilva, A. G., Conant, K. and Yong, V. W. (2006). Myelin formation during development of the CNS is delayed in matrix metalloproteinase-9 and -12 null mice. *J. Neurosci.* **26**, 2207-2214.
Lewallen, K. A., Shen, Y.-A. A., De La Torre, A. R., Ng, B. K., Meijer, D. and Chan, J. R. (2011). Assessing the role of the cadherin/catenin complex at the Schwann cell-axon interface and in the initiation of myelination. *J. Neurosci.* **31**, 3032-3043.
Li, H., He, Y., Richardson, W. D. and Casaccia, P. (2009). Two-tier transcriptional control of oligodendrocyte differentiation. *Curr. Opin. Neurobiol.* **19**, 479-485.
Louis, S. A., Mak, C. K. H. and Reynolds, B. A. (2013). Methods to culture, differentiate, and characterize neural stem cells from the adult and embryonic mouse central nervous system. *Methods Mol. Biol.* **946**, 479-506.
Lu, Q. R., Yuk, D.-i., Alberta, J. A., Zhu, Z., Pawlitzky, I., Chan, J., McMahon, A. P., Stiles, C. D. and Rowitch, D. H. (2000). Sonic hedgehog–regulated oligodendrocyte lineage genes encoding bHLH proteins in the mammalian central nervous system. *Neuron* **25**, 317-329.
Massagué, J. (2012). TGFbeta signalling in context. *Nat. Rev. Mol. Cell Biol.* **13**, 616-630.
McKinnon, R. D., Piras, G., Ida, J. A., Jr and Dubois-Dalcq, M. (1993). A role for TGF-beta in oligodendrocyte differentiation. *J. Cell Biol.* **121**, 1397-1407.
Mecha, M., Rabadan, M. A., Peña-Melián, A., Valencia, M., Mondéjar, T. and Blanco, M. J. (2008). Expression of TGF-betas in the embryonic nervous system: analysis of interbalance between isoforms. *Dev. Dyn.* **237**, 1709-1717.
Mekki-Dauriac, S., Agius, E., Kan, P. and Cochard, P. (2002). Bone morphogenetic proteins negatively control oligodendrocyte precursor specification in the chick spinal cord. *Development* **129**, 5117-5130.
Meyerheim, H. L., Sander, D., Popescu, R., Kirschner, J., Robach, O. and Ferrer, S. (2004). Spin reorientation and structural relaxation of atomic layers: pushing the limits of accuracy. *Phys. Rev. Lett.* **93**, 156105.
Miguez, D. G., Gil-Guinon, E., Pons, S. and Marti, E. (2013). Smad2 and Smad3 cooperate and antagonize simultaneously in vertebrate neurogenesis. *J. Cell Sci.* **126**, 5335-5343.
Miller, R. H., Dinsio, K., Wang, R., Geertman, R., Maier, C. E. and Hall, A. K. (2004). Patterning of spinal cord oligodendrocyte development by dorsally derived BMP4. *J. Neurosci. Res.* **76**, 9-19.
Miron, V. E., Boyd, A., Zhao, J.-W., Yuen, T. J., Ruckh, J. M., Shadrach, J. L., van Wijngaarden, P., Wagers, A. J., Williams, A., Franklin, R. J. et al. (2013). M2 microglia and macrophages drive oligodendrocyte differentiation during CNS remyelination. *Nat. Neurosci.* **16**, 1211-1218.
Montag, D., Giese, K. P., Bartsch, U., Martini, R., Lang, Y., Blüthmann, H., Karthigasan, J., Kirschner, D. A., Wintergerst, E. S., Nave, K.-A. et al. (1994). Mice deficient for the myelin-associated glycoprotein show subtle abnormalities in myelin. *Neuron* **13**, 229-246.
Muñoz-Sanjuán, I. and Brivanlou, A. H. (2002). Neural induction, the default model and embryonic stem cells. *Nat. Rev. Neurosci.* **3**, 271-280.
Nolan, E. M., Jaworski, J., Okamoto, K.-I., Hayashi, Y., Sheng, M. and Lippard, S. J. (2005). QZ1 and QZ2: rapid, reversible quinoline-derivatized fluoresceins for sensing biological Zn(II). *J. Am. Chem. Soc.* **127**, 16812-16823.
Ono, K., Bansal, R., Payne, J., Rutishauser, U. and Miller, R. H. (1995). Early development and dispersal of oligodendrocyte precursors in the embryonic chick spinal cord. *Development* **121**, 1743-1754.
Orentas, D. M. and Miller, R. H. (1996). The origin of spinal cord oligodendrocytes is dependent on local influences from the notochord. *Dev. Biol.* **177**, 43-53.
Poulsen, K. T., Armanini, M. P., Klein, R. D., Hynes, M. A., Phillips, H. S. and Rosenthal, A. (1994). TGF beta 2 and TGF beta 3 are potent survival factors for midbrain dopaminergic neurons. *Neuron* **13**, 1245-1252.
Raff, M. C., Lillien, L. E., Richardson, W. D., Burne, J. F. and Noble, M. D. (1988). Platelet-derived growth factor from astrocytes drives the clock that times oligodendrocyte development in culture. *Nature* **333**, 562-565.
Richardson, W. D., Kessaris, N. and Pringle, N. (2006). Oligodendrocyte wars. *Nat. Rev. Neurosci.* **7**, 11-18.
Ridley, A. J., Davis, J. B., Stroobant, P. and Land, H. (1989). Transforming growth factors-beta 1 and beta 2 are mitogens for rat Schwann cells. *J. Cell Biol.* **109**, 3419-3424.
Schubert, D., Kimura, H., LaCorbiere, M., Vaughan, J., Karr, D. and Fischer, W. H. (1990). Activin is a nerve cell survival molecule. *Nature* **344**, 868-870.
Schulz, R., Vogel, T., Dressel, R. and Krieglstein, K. (2008). TGF-beta superfamily members, ActivinA and TGF-beta1, induce apoptosis in oligodendrocytes by different pathways. *Cell Tissue Res.* **334**, 327-338.
Schwammenthal, E., Popescu, B. A., Popescu, A. C., Di Segni, E., Guetta, V., Rath, S., Eldar, M. and Feinberg, M. S. (2004). Association of left ventricular filling parameters assessed by pulsed wave Doppler and color M-mode Doppler echocardiography with left ventricular pathology, pulmonary congestion, and left ventricular end-diastolic pressure. *Am. J. Cardiol.* **94**, 488-491.
See, J., Zhang, X., Eraydin, N., Mun, S.-B., Mamontov, P., Golden, J. A. and Grinspan, J. B. (2004). Oligodendrocyte maturation is inhibited by bone morphogenetic protein. *Mol. Cell. Neurosci.* **26**, 481-492.

Development (2014) 141, 2414-2428 doi:10.1242/dev.106492

Shi, Y. and Massagué, J. (2003). Mechanisms of TGF-beta signaling from cell membrane to the nucleus. *Cell* **113**, 685-700.

Stern, C. D., Yu, R. T., Kakizuka, A., Kintner, C. R., Mathews, L. S., Vale, W. W., Evans, R. M. and Umesono, K. (1995). Activin and its receptors during gastrulation and the later phases of mesoderm development in the chick embryo. *Dev. Biol.* **172**, 192-205.

Stolt, C. C., Lommes, P., Sock, E., Chaboissier, M.-C., Schedl, A. and Wegner, M. (2003). The Sox9 transcription factor determines glial fate choice in the developing spinal cord. *Genes Dev.* **17**, 1677-1689.

Vassalli, A., Matzuk, M. M., Gardner, H. A., Lee, K. F. and Jaenisch, R. (1994). Activin/inhibin beta B subunit gene disruption leads to defects in eyelid development and female reproduction. *Genes Dev.* **8**, 414-427.

Yang, X., Letterio, J. J., Lechleider, R. J., Chen, L., Hayman, R., Gu, H., Roberts, A. B. and Deng, C. (1999). Targeted disruption of SMAD3 results in impaired mucosal immunity and diminished T cell responsiveness to TGF-beta. *EMBO J.* **18**, 1280-1291.

Yim, S. H., Hammer, J. A. and Quarles, R. H. (2001). Differences in signal transduction pathways by which platelet-derived and fibroblast growth factors activate extracellular signal-regulated kinase in differentiating oligodendrocytes. *J. Neurochem.* **76**, 1925-1934.

Zhang, Y., Taveggia, C., Melendez-Vasquez, C., Einheber, S., Raine, C. S., Salzer, J. L., Brosnan, C. F. and John, G. R. (2006). Interleukin-11 potentiates oligodendrocyte survival and maturation, and myelin formation. *J. Neurosci.* **26**, 12174-12185.

Zhang, Y., Argaw, A. T., Gurfein, B. T., Zameer, A., Snyder, B. J., Ge, C., Lu, Q. R., Rowitch, D. H., Raine, C. S., Brosnan, C. F. et al. (2009). Notch1 signaling plays a role in regulating precursor differentiation during CNS remyelination. *Proc. Natl. Acad. Sci. U.S.A.* **106**, 19162-19167.

Zhang, J., Zhang, Y., Dutta, D. J., Argaw, A. T., Bonnamain, V., Seto, J., Braun, D. A., Zameer, A., Hayot, F., Lopez, C. B. et al. (2011). Proapoptotic and antiapoptotic actions of Stat1 versus Stat3 underlie neuroprotective and immunoregulatory functions of IL-11. *J. Immunol.* **187**, 1129-1141.